ELUCIDATION OF LYSOSOMAL CATHEPSIN A IN THE REGULATION OF AUTOPHAGY

A Thesis Submitted to the
Graduate School of Engineering and Sciences of
İzmir Institute of Technology
in Partial Fulfillment of the Requirements for the Degree of

MASTER OF SCIENCE

in Molecular Biology and Genetics

by Selman YANBUL

July 2023

İzmir

We approve the thesis of **Selman YANBUL**

Examining Committee Members:

Prof. Dr. Volkan SEYRANTEPE
Department of Molecular Biology and Genetics, Izmir Institute of Technology

Prof. Dr. Özden YALÇIN ÖZUYSAL
Department of Molecular Biology and Genetics, Izmir Institute of Technology

Prof. Dr. Şermin GENÇ
Department of Molecular Biology and Genetics, Izmir Biomedicine and Genome Center, Dokuz Eylül University

14 July 2023

Prof. Dr. Volkan SEYRANTEPE
Supervisor, Department of Molecular Biology and Genetics
Izmir Institute of Technology

Prof. Dr. Özden YALÇIN ÖZUYSAL
Head of Department of Molecular Biology and Genetics

Prof. Dr. Mehtap EANES
Dean of Graduate School of Engineering and Science

ACKNOWLEDGEMENTS

First of all, I would like to express my sincere thanks and deepest gratitude to my supervisor, Prof. Dr. Volkan SEYRANTEPE. He has supported and encouraged me both academically and scientifically since my undergraduate years, he always showed understanding towards me and guided and helped me with his extensive knowledge and experience throughout my thesis studies.

I would like to express my heartfelt thanks to Prof. Dr. Özden YALÇIN ÖZUYSAL and Prof. Dr. Şermin GENÇ for their kind help and guidance during my thesis study.

I am also thankful to The Scientific and Technological Research Council of Turkey (TUBITAK) for their partial financial support of this thesis study and for providing me the scholarship.

I also would like to express my sincere thanks to my co-workers Orhan Kerim İNCİ, Nurselin ATEŞ, Tuğçe ŞENGÜL, İlker GÜMÜŞ, Tufan Utku ÇALIŞKAN, Melike CAN ÖZGÜR, Hatice Hande BASIRLI, Beyza KAYA, and Ebru ADA for their supports, helps and assistances during my thesis studies and research. I would also like to thank Orhan Kerim İNCİ for his sincere and reliable friendship and neighborliness. I would like to thank Seçil AKYILDIZ DEMİR, who supported and mentored me both technically and theoretically throughout my graduate studies. I am also thankful to undergraduate members of the Seyrantepe Laboratory for their sincere help and kindness.

Finally, I would like to send the biggest and most special thanks to my father Mustafa YANBUL, my mother Fidan YANBUL, and my sister Yasemin YANBUL for their endless love, belief, motivation, support, and encouragement throughout my whole life. My dear family, I would never have gotten to where I am today without you, and I would not have accomplished anything I have accomplished so far.

ABSTRACT

ELUCIDATION OF LYSOSOMAL CATHEPSIN A IN THE REGULATION OF AUTOPHAGY

Lysosomal Cathepsin A (CathA) is a multifunctional enzyme with independent catalytic and protective functions. It has a serine carboxypeptidase activity in acidic pH conditions for the degradation of short bioactive peptides that are vasoactive peptides including endothelin-1, angiotensin-I, bradykinin and neuropeptides including oxytocin and substance P. Lysosomal CathA enzyme also forms a lysosomal multienzyme complex (LMC) with α-neuraminidase (Neu1) and ß-Galactosidase (ß-Gal) enzymes to protect them from hydrolytic degradation in lysosomes and due to its protective function. Genetic defects in the lysosomal CathA enzyme causes a rare lysosomal storage disorder, Galactosialidosis (OMIM #256540), with secondary deficiencies of Neu1 and ß-Gal enzymes. Catalytically inactive Cathepsin A knock-in mouse model, $CathA^{S190A}$ has point mutation in the active catalytic site which serine was replace with alanine amino acid. Accumulation of short bioactive peptides has been reported in previous studies in different tissues of the $CathA^{S190A}$ mouse model. In this thesis study, investigation the role of the lysosomal CathA enzyme in the regulation of autophagic flux in neuroglia and fibroblast cell lines derived from $CathA^{S190A}$ mice was aimed. For this aim; RT-PCR, Western Blot and Immunocytochemical analyses were for performed for autophagy markers. Thesis study results have exhibited that catalytically deficient CathA causes the impairment in autophagic machinery with secondary accumulation of autophagic substrates and alterations in the expression of the autophagy marker genes. Accumulation of the short bioactive peptides due to the catalytically inactive CathA enzyme may be related to to impaired autophagic flux. Autophagy-inducing Rapamycin and Starvation treatment conditions may restore the impaired autophagic flux due to catalytically inactive CathA enzyme with the clearance of accumulation of secondary autophagic substrates.

ÖZET

LİZOZOMAL KATEPSİN A'NIN OTOFAJİNİN DÜZENLENMESİNDEKİ ROLÜNÜN ARAŞTIRILMASI

Lizozomal Katepsin A (CathA), birbirinden bağımsız katalitik ve koruyucu işlevlere sahip çok işlevli bir enzimdir. Lizozomal Katepsin A enzimi, asidik pH koşullarında, vazoaktif peptidler olan endotelin-1, anjiyotensin-1 ve bradikinin ve nöropeptidler olan oksitozin ve substans P'ye karşı hidrolitik aktiviteye sahiptir. Ayrıca Lizozomal CathA enzimi, α-nöraminidaz (Neu1) ve ß-Galaktosidaz (ß-Gal) enzimleri ile lizozomal multienzim kompleksi oluşturarak bu enzimlerin lizozomlarda hidrolitik bozunmadan korur. Lizozomal CathA enzimindeki mutasyonlar, Neu1 ve ß-Gal enzimlerinin sekonder eksiklikleriyle birlikte nadir görülen bir lizozomal depolanma bozukluğu olan Galaktosiyalidoza (OMIM #256540) neden olur. Katalitik olarak aktif olmayan Cathepsin A knock-in fare modeli, $CathA^{S190A}$, aktif katalitik bölgede serinin alanin amino asitle değiştirildiği nokta mutasyonuna sahiptir. $CathA^{S190A}$ fare modelinin farklı dokularında önceki çalışmalarda kısa biyoaktif peptidlerin birikimi gösterilmiştir. Bu tez çalışmasında, $CathA^{S190A}$ farelerinden türetilen nöroglia ve fibroblast hücre hatlarında otofajik akışın düzenlenmesinde lizozomal CathA enziminin rolünün araştırılması amaçlanmıştır. Bu amaçla; otofaji belirteçleri için RT-PCR, Western Blot ve İmmunositokimyasal analizler yapıldı. Tez çalışması sonuçları, katalitik olarak eksik olan CathA'nın, otofajik substratların ikincil birikimi ve otofaji işaretleyici genlerin ekspresyonundaki değişiklikler ile otofajik mekanizmada bozulmaya neden olduğunu göstermiştir. Katalitik olarak aktif olmayan CathA enzimi nedeniyle kısa biyoaktif peptitlerin birikmesi, bozulmuş otofajik akı ile ilişkili olabilir. Otofajiyi indükleyen Rapamisin ve Açlık tedavi koşulları, ikincil otofajik substratların birikiminin temizlenmesiyle katalitik olarak inaktif CathA enzimi nedeniyle bozulmuş otofajik akışı geri döndürebilir.

TABLE OF CONTENTS

LIST OF FIGURES

Figure **Page**

Figure **Page**

LIST OF TABLES

Table **Page**

CHAPTER 1

INTRODUCTION

1.1. Lysosome

Lysosomes, as a mean of "lytic bodies", was firstly discovered and introduced in rat liver as new cytoplasmic members by de Duve in 1955 (de Duve et al., 1955). Lysosomes are cytoplasmic organelles found in eukaryotic cells which are enclosed by membranes and contain several hydrolytic enzymes. These hydrolytic enzymes, hydrolases, are soluble and work in acidic pH values and they play a role to maintain cellular homeostasis by hydrolyzing the macromolecules (de Duve et al., 1955; de Duve et al., 1959).

Lysosomes contain hydrolases to degrade the biological materials which were taken from outside the cell (extracellular) or inside the cell (intracellular). Extracellular biological materials are hydrolyzed using the endocytosis pathway, intracellular biological materials are also hydrolyzed using the autophagy mechanism and both of the cellular events are finalized in lysosomes. Endocytosis is the internalization of the components or cargoes from the plasma membrane and the degradation of those internalized components in lysosomes. Lipids and integral proteins of the plasma membrane and extracellular environment work in harmony to invaginate the extracellular components and invaginated components are routed to the lysosome in the specific compartments, called as "endosomes". On the other hand, autophagy is the degradation and recycling of the cell's own components. Dysfunctional, misfolded, or half-aged macromolecules, long-lived organelles, etc. are subjected to the lysosome in membraneous vesicles or in non-membranous ways for their degradation by using autophagy mechanism in the cell. Both of these lysosome-routed cellular mechanisms, endocytosis and autophagy are interconnected with each other (Birgisdottir and Johansen, 2020).

More than 50 hydrolase enzymes have been identified so far which are proteases, glycosidases, phosphatases, nucleases, sulfatases, and lipases. Most of the lysosomal acid

hydrolases are synthesized in ribosomes of the rough Endoplasmic Reticulum (ER) as proenzyme. Synthesized proenzymes are directed to the lumen of the ER and then, they are translocated to the Golgi apparatus via ER-Golgi intermediate compartment. In the cis-Golgi compartment, the mannose residue of the enzymes is phosphorylated to form mannose 6-phosphate (M6P). This phosphorylation is required to routing of the enzyme to the lysosome via M6P receptors that direct the enzymes to the endo-lysosomal pathway by late endosome vesicles. These clathrin-coated endosomal vesicles arrive at lysosomes and hydrolase enzymes are separated from M6P receptors and then released into the lysosomes where they are enzymatically active (Braulke and Bonifacino, 2009).

Lysosomes have a vital role in cells and failures in the lysosomes or digestive lysosomal hydrolases lead to several diseases which are known as lysosomal storage disorders (LSDs). More than 70 different LSD have been identified so far and most of the disorders are single-gene disorders and inherited as autosomal recessively. LSDs are caused by mutations in genes that encode the lysosomal enzymes or proteins and these mutations lead to accumulation of substrates in the lysosome. LSDs are rarely seen diseases and affect 1/5000 births on average. Most severe forms of LSDs are faced in infancy or childhood (early-onset) and also some LSD patients are classified as adult-onset. These groups of disorders mainly affect the central nervous system (CNS), and peripheral organs such as kidney, liver, lungs, etc. and they show progressive neurodegeneration in patients (Platt et al., 2018).

1.2. Lysosomal Proteases

Proteases are a group of enzymes in lysosomes that have a pivotal role in the degradation of proteins or peptides into the building blocks. As a first, proteases had been mentioned by Levene PA in 1905. Alongside the degradation of peptides into amino acids, proteases are required in specialized reactions of proteolytic events and handling of the new proteins. Proteases are included in a bunch of cellular activities such as regulation of protein-protein interaction, replication and transcription of DNA, proliferation, and differentiation of cells, neurogenesis, fertilization etc. They are classified into six subgroups according to the catalytic group of active sites: threonine proteases, cysteine proteases, aspartic proteases, metalloproteases, glutamic proteases, and serine proteases such as Cathepsin A (López-Otín and Bond, 2008).

Lysosomal proteases are serine, cysteine, or aspartic protease family. Their expression patterns differ from tissue to tissue or from cell to cell. Proteases work as gears of a machine in the process of proteolytic degradation. In addition to their main functions of protein or peptide degradation, lysosomal proteases are involved in the processing of antigens in endosomes, initiation of programmed cell death mechanism apoptosis, processing of hormones, and digestion of the cellular matrix components in extracellular space (Brix, 2005).

1.3. Cathepsin Enzyme Family

Cathepsins are protease enzymes that are generally located in highly acidic lysosomes and could be secreted out of the cell. As an addition to their proteolytic functions, Cathepsins can play a role in several cellular activities such as antigen processing in immune response, degradation of chemokines, etc. The Cathepsin family is divided into the 3 subfamily depending on the amino acid in their active sites that are serine protease Cathepsins (Cathepsin A and G), cysteine protease Cathepsins (Cathepsin B, C, F, H, K, L, O, S, V, X, and W) and aspartic protease Cathepsins (Cathepsin D and E) (Table 1.1). Their highest enzymatic activity is shown in acidic pH conditions but some Cathepsins have a broad spectrum of enzymatic activity in changing pH conditions in and out of the cell. Expression and localization patterns of Cathepsins vary from tissue to tissue or cell type to cell type. Dysregulated or mutated Cathepsin expression and enzymatic activity is associated with several diseases with clinical symptoms such as inflammatory neurological disorders, neurodegenerative diseases, cardiovascular disorders, and cancer. For example, a deficiency of lysosomal Cathepsin A leads to a rare type of LSD, Galactosialidosis (Yadati et al., 2020).

Table 1.1: Cathepsin protease subfamilies and members

	Cathepsin Enzymes
Serine Protease Cathepsins	Cathepsin A and G
Cysteine Protease Cathepsins	Cathepsin B, C, F, H, K, L, O, S, V, X, and W
Aspartic Protease Cathepsins	Cathepsin D and E

1.4. Lysosomal Cathepsin A (CathA)

Lysosomal Cathepsin A (CathA) is a member of the serine protease family which has carboxypeptidase, deamidase, and esterase activity in different pH conditions, and CathA enzyme is encoded by *CTSA* gene. It has a highly similar homology as structural with yeast carboxypeptidase Y (Hiraiwa, 1999). Besides its catalytic activities, it constitutes a lysosomal multienzyme complex (LMC) with ß-galactosidase (ß-Gal) and α-neuraminidase (Neu1) to protect them from hydrolytic degradation in lysosomes. Thanks to this protective function, it is also known as Protective Protein/Cathepsin A (PPCA). Although Cathepsin A enzyme can form another enzymatic complex, cell surface elastin receptor (CSER), on the plasma membrane with Neu1 and elastin-binding protein (EBP) to involve and regulate elastic fiber formation. The catalytic and protective functions of Cathepsin A are distinct from each other. Lysosomal Cathepsin A is produced as 54 kDa one-chain proenzyme. This proenzyme is cleaved into the two-chain (32/20 kDa) mature and active form of lysosomal CathA by an extraordinary proteolysis mechanism (Bonten et al., 2014).

Lysosomal Cathepsin A is a serine carboxypeptidase enzyme within the pH 4.5.-5.5 and it has also esterase and deamidase activities in neutral pH conditions. Lysosomal Cathepsin A enzyme is able to degrade short bioactive peptides that are vasoactive peptides including endothelin-1, angiotensin-I, bradykinin, and neuropeptides including oxytocin and substance P (Bonten et al., 2014). Endothelin-1 (ET-1) is 21 amino acids vasoconstrictor peptide and plays a role in the regulation of blood pressure. ET-1 is highly abundant in the cardiovascular system and highly expressed in especially vascular endothelium but several cell types in the human body can express ET-1 such as epithelial cells, macrophages, astrocytes, microglias, oligodendrocytes, neurons, kidney and lung cells, etc (Davenport et al., 2016). This peptide is inhibited by CathA from its carboxy terminus. Cathepsin A deficient human galactosialidosis patients' fibroblast cells and autopsied patients' brains show high amounts of ET-1 abundance (Itoh et al., 2000). As an addition to this study; catalytically inactive Cathepsin A knock-in mouse model, $CathA^{S190A}$, and Scpep1, Cathepsin A homolog, double deficient mouse model $CathA^{S190A}/Scpep1^{-/-}$ has shown a significantly high level of ET-1 in lung and blood plasma compared to age-matched WT (Pan et al., 2014). Oxytocin is 9 aa neuropeptide and plays a role in the processing of mammalian social relationships and acts. This

neuropeptide is highly expressed in pervo- and magnocellular neurons in the paraventricular nucleus of the hypothalamus but its receptors are highly abundant in the hippocampus region of mammalian brains (Breton and Zingg, 1997; Rocicki et al., 2022).

Lysosomal CathA associates with Neu1 and ß-Gal glycosidases to form a lysosomal multienzyme complex to prevent these enzymes in highly acidic lysosomes (Figure 1.1). Neu1 and ß-Gal glycosidases are involved in glycolipid and glycoprotein degradation. Neu1 is a sialidase enzyme that is encoded by *NEU1* gene in humans, it cleaves the sialic acid residues in the glycoconjugates, and *GLB1* gene product ß-Gal enzyme removes galactose moieties from glycoproteins and glycolipids. Lysosomal CathA is required for the transport, activation, and stabilization of the Neu1 enzyme and it increases the enzymatic half-life of ß-Gal enzyme (Gorelik et al., 2021). Defects in the lysosomal Cathepsin A enzyme result in glycoprotein storage disorder, Galactosialidosis (GS) (OMIM #256540), with secondary complete deficiency of Neu1 and partial deficiency of ß-Gal enzymes (~15–20% enzymatic activity) (Gorelik et al., 2021). GS is a very rare and recessively inherited disease, also its clinical symptoms are very similar to sialidosis (OMIM #256550) which is caused by mutations in the Neu1 enzyme. Galactosialidosis reflects typical features of LSDs with coarse face, hydrops fetalis, vision and hearing loss, seizures, cognitive disabilities, etc. Galactosialidosis is classified into the 3 subtypes according to the age of onset and symptoms severity which are early infantile GS, late infantile GS, and juvenile/adult form of GS. The most severe form of GS is the early infantile form and patients start to show symptoms between birth to 3-months old of age. Early infantile GS patients also develop visceromegaly, cardiac and renal failures and they die within 1 year of age mostly caused by heart and kidney abnormalities (Annunziata and d'Azzo, 2017)

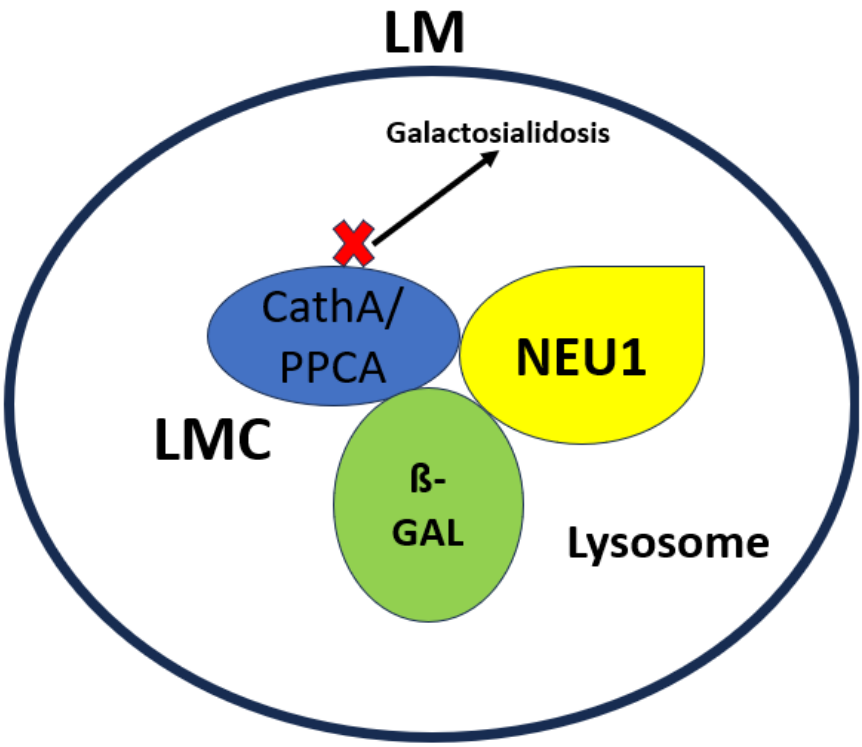

Figure 1.1: Representative schematic illustration of lysosomal multienzyme complex

1.5. Cathepsin A Animal Models

To study the molecular functions of lysosomal CathA and the pathophysiology of Galactosialidosis, two different mouse models of lysosomal CathA have been generated: CathA knock-in mice (*CathA*^{S190A}) and CathA knock-out mice (*CathA*$^{-/-}$), respectively (Annunziata and d'Azzo, 2017).

CathA$^{-/-}$ mouse model is homozygous knocked-out for the null mutation at *Ctsa* gene region which encodes Cathepsin A enzyme. Both of the functions of lysosomal Cathepsin A, protective and catalytic functions, are blocked in this mouse model and nearly zero Cathepsin A activity is observed. This mouse model presents the symptoms of an early infantile form of GS and secondary complete deficiency of Neu1 enzymatic activity and partial deficiency of ß-Gal enzymes are seen in this mouse model. Lysosomal vacuolation and expansion in the cells of some peripheral organs and the central nervous system are seen in the first week after the birth in *CathA*$^{-/-}$ mouse model. When the disease progresses, pathological changes could be detected in the reticuloendothelial system of mice, splenomegaly, cardiac system failures, and oligosaccharidurie that is caused by secondary deficiency of Neu1 enzyme. *CathA*$^{-/-}$ male mice are infertile because of impaired sperm mobility resulting from some dysregulations in the blood-epididymal

barrier. This knock-out mouse model has a reduced life span, and generally dies between 6-9 months of age (Annunziata and d'Azzo, 2017).

CathA^{S190A} is a catalytically inactive knock-in mouse model in that serine amino acid was replaced with alanine amino acid in the active catalytic domain of CathA enzyme coding sequence in *Ctsa* gene. On the other hand, the protective function of lysosomal CathA is preserved in this mouse model, so the lysosomal CathA enzyme in *CathA*^{S190A} mice is able to form LMC with Neu1 and ß-Gal glycosidases. Because of the capable of *CathA*^{S190A} forming a LMC, secondary deficiencies of Neu1 and ß-Gal enzymes are not seen, and both of these enzymes show catalytic activity in the fractions of tissues which are obtained from *CathA*^{S190A} mice. A targeted point mutation in the active site of the CathA enzyme in *CathA*^{S190A} mice resulted in nearly zero carboxypeptidase activity of CathA enzyme but immunohistochemical staining, Western Blot, and Northern Blot results showed the presence of CathA enzyme in protein and mRNA levels. Catalytically inactive *CathA*^{S190A} mice are fertile, sign no developmental defect, and a normal life span is seen in this mouse model (Seyrantepe et al., 2008).

The inhibitory role of CathA enzyme on the short bioactive peptides (endothelin-1, angiotensin-I, bradykinin, oxytocin, and substance P) is shown *in vitro* studies (Jackman et al., 1990; Jackman et al., 1992). Also, *in vivo* role of lysosomal CathA in the degradation of short bioactive peptides was shown in catalytically inactive *CathA*^{S190A} male mice. Enzyme-linked immunosorbent assay (ELISA) results in 3- and 6-month-old *CathA*^{S190A} mice and their age-matched WT littermates concluded accumulation of short bioactive peptides in kidney, liver, lung, brain tissue lysates and in serum because of the deficiency of the catalytic activity of lysosomal CathA enzyme (Timur et al., 2016). Also, hippocampal accumulations of endothelin-1 and oxytocin in 3-, 6- and 12-month-old *CathA*^{S190A} mice compared to WT were presented using the immunohistochemical staining method. In relation to this accumulation in the hippocampus region of *CathA*^{S190A} mice brains, some neurobehavioral abnormalities are reported in *CathA*^{S190A} mice such as impairment in learning and long-term memory (Calhan and Seyrantepe, 2017).

1.6. Autophagy

Autophagy is the cellular degradation pathway of the macromolecules, organelles, pathogens, etc. to maintain cellular homeostasis that is taken place in the lysosome of all eukaryotes. The autophagy mechanism is used to recycle long-lived or non-mandatory macromolecules into building blocks to provide a source for newly synthesized macromolecules or to obtain energy sources under stress conditions. Also, this cellular degradation pathway is highly required for the digestion of damaged or superfluous organelles such as mitochondria (mitophagy), peroxisome (pexophagy), lysosome (lysophagy), etc. Three primary types of autophagy have been identified that are macroautophagy, microautophagy, and chaperone-mediated autophagy (CMA) and all three autophagy types are finalized in highly acidic lysosome (Figure 1.2). Macroautophagy required a membranous structure, which is called as "autophagosome" to deliver cytoplasmic cargo to the lysosome, on the contrary, any membranous vesicle is not involved in microautophagy and CMA. Unless otherwise stated, autophagy refers to macroautophagy (Feng et al., 2014; Yang and Klionsky, 2010; Parzych and Klionsky, 2014).

Autophagy is tightly regulated in cells; some intra- or extracellular stresses and conditions may lead to upregulation or downregulation of autophagic flux to maintain cellular homeostasis and dysregulation of autophagy has a role in the pathology of several diseases such as neurodegeneration, cancer, and infectious diseases. Starvation, nutrient or growth factor deprivation, and infection of cells by pathogen result in the upregulation of autophagy in cells. Also, several chemical agents are used to regulate autophagy (He and Klionsky, 2009). Rapamycin is one of the well-known inducers of autophagy that inhibits the mTOR complex and it is widely used to reverse impaired autophagic machinery (Sarkar et al., 2009). Earle's Balanced Salt Solution (EBSS) is a nutrient-free cell culture medium to induce autophagy by mimicking and triggering starvation condition (Min et al., 2013). Starvation-induced autophagy for the clearance of accumulated substrates was one of the used therapy models in several lysosomal storage disorders such as Niemann-Pick and Fabry diseases (Sarkar et al., 2013; Lieberman et al., 2012).

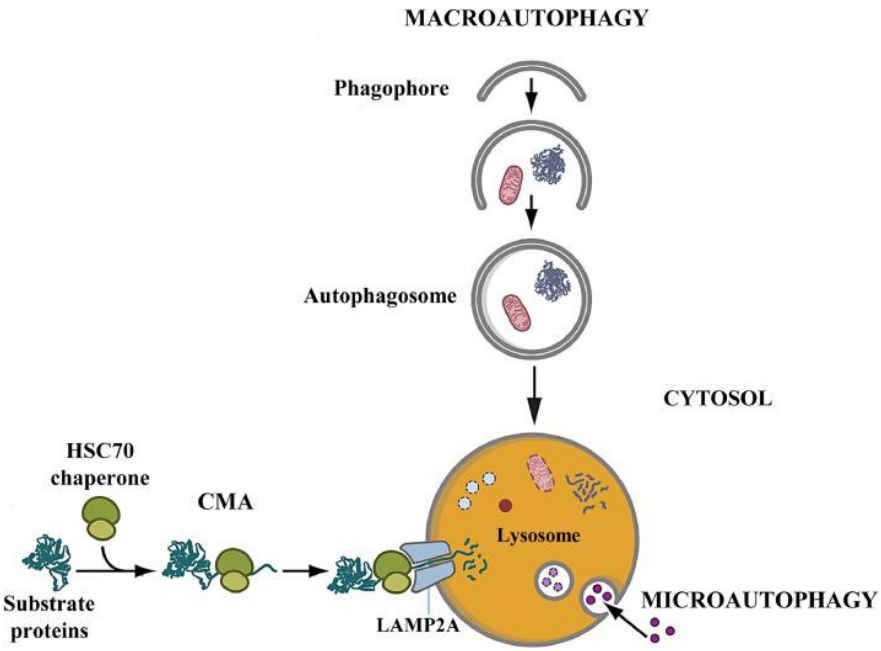

Figure 1.2: Three types of autophagy (Source: Myerowitz et al., 2021).

In the autophagic machinery, as a first, the cytoplasmic content will be degraded, environed by phagophore structure that double-membrane intracellular structure. Then, the double-membrane phagophore is expanded and closed to generate an autophagosome structure. Formed autophagosome structure docks and fuses with the lysosome to form an autophagosome where acidic hydrolytic degradation occurs. Several proteins, enzymes, and protein or enzyme complexes have a crucial role in this tightly regulated cellular event (Figure 1.3) (Misuzhima et al., 2002; Feng et al, 2014).

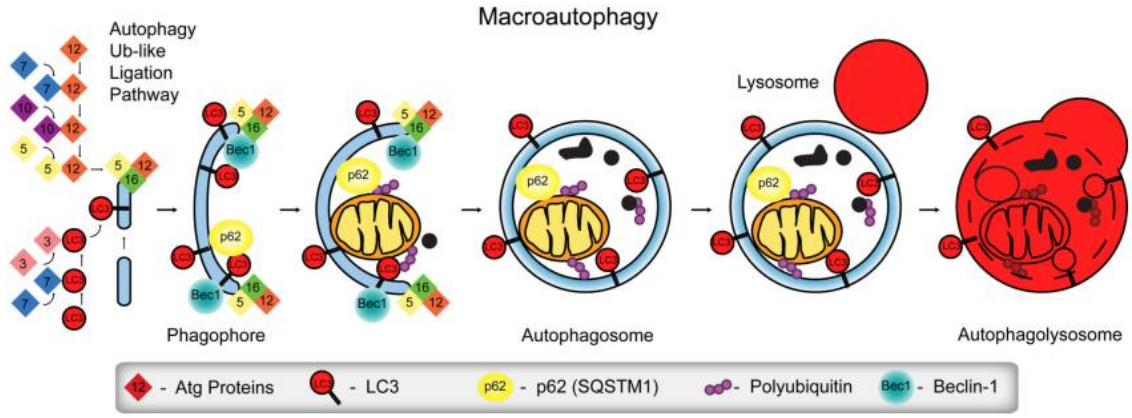

Figure 1.3: Representative schematic presentation of the macroautophagy pathway (Source: Gump and Thorburn, 2011).

Numerous proteins, enzymes, and protein or enzyme complexes have crucial roles in the regulation of autophagic flux. One of the core components of autophagic flux regulation is autophagy-related (Atg) genes proteins/enzymes which have been primarily worked on yeast organisms. The discovery of Atg proteins has led to a shifting of the autophagy study perspective from the morphology to the molecular level. Atg proteins are found in the nucleation/initiation, elongation, and termination steps of autophagy. A group of Atg proteins is crucially involved in autophagosome formation and so, they are termed as "the core autophagy machinery": (i) Atg1/ULK complex, (ii) transmembrane Atg9 system, (iii) the PtdIns3-kinase (PtdIns3K) complex and (iv) two ubiquitin-like proteins, Atg8/LC3 and Atg12. These four core autophagy machinery complexes are routed to the phagophore assembly site (PAS) where autophagosome formation begins (Yang and Klionsky, 2010; Feng et al., 2014). Atg1, Atg11, Atg13, Atg17, Atg29, and Atg31 are involved in Atg1/ULK complex which is the primary complex for autophagosome formation induction and its regulation in yeast. In mammalian cells, ULK1/2 complex is consisted of ULK1/2 (Atg1 mammalian homolog), ATG13 (Atg13 mammalian homolog), C12orf44/ATG101 and RB1CC1/FIP200 (Atg17 mammalian homolog). ULK1 kinase would be activated in 2 ways: AMP-activated protein kinase-dependent (senses glucose starvation) and independent (senses amino acid starvation). In nutrient-rich conditions, the mammalian target of rapamycin complex 1 (mTORC1) inhibits the ULK1/2 complex by phosphorylating it and prevents AMP-activated protein kinase interaction with the ULK1/2 complex. In contrast, mTORC1 is no longer able to interact with the ULK1/2 complex, and therefore ULK1/2 complex is activated in mammalian cells under nutrient deficiency or starvation (Feng et al., 2014; Laplante and Sabatini, 2013). Also dephosphorylated ULK1/2 complex activates by phosphorylating AMBRA1 and Beclin-1 proteins which are the members of the PtdIns3K complex. Activation of PtdIns3K complex members leads to the recruitment of lipid kinase Vps-proteins complex into the ER to form the lipid bilayer of the autophagosome (Feng et al., 2014; Russell et al., 2013).

ATG9 is a transmembrane protein where localized in small vesicles in the *trans*-Golgi network and it has a multifunctional role in autophagic machinery. ATG9 has a cycling system; transporting of ATG9 from the *trans*-Golgi network to the PAS is regulated by ATG11, ATG23, and ATG27, and anterograde transport of serving ATG9s into the initial site where they are stored, is also regulated by ATG1, ATG2, ATG13, and ATG18. ATG9 recruits the lipids from donor sources which are required for

autophagosome formation and transporting them into PAS. In addition to the role of lipid transferring to the forming autophagosome, ATG9 acts like a membrane scaffold during the autophagosome formation (Feng et al., 2014; Mari et al., 2011; Orsi et al., 2010).

Nucleation of the phagophore and autophagosome assembly is followed by autophagosome membrane elongation/expansion by the Ub1 protein conjugation system. LC3 (mammalian ortholog of yeast Atg8), known as MAP1LC3, is recruited to the autophagosome membrane and plays a role in autophagosome formation, elongation, and fusion with lysosomes. LC3 protein is modified post-translationally; ATG4B cuts the glycine amino acid in the C-terminal of pro-LC3 for the forming of LC3-I which is a cytosolic form of LC3. Cytosolic LC3-I is converted to the autophagosome-associated form of LC3, LC3-II, with the addition of phosphatidylethanolamine (PE) to its C-terminus. The E1-like enzyme, ATG7 (mammalian ortholog of yeast Atg7), has a role in the conjugation of the PE to LC3-I to form LC3-II. Also, ATG7 is involved in the ATG5-ATG12 conjugation system. LC3 is frequently used to monitor autophagic flux, activity, and level of the organisms in healthy or disease state (Feng et al., 2014; Mizushima et al., 2011; Tanida et al., 2004).

p62, also called as SQSTM1/p62, is a multifunctional protein that has a pivotal role in autophagy. p62 is responsible for recognizing and targeting ubiquitinated cargo to the autophagosome by interacting with the autophagosome membrane-associated LC3-II. Additionally, studies have revealed that p62 is degraded through the autophagy-lysosomal pathway. This is also called selective autophagy since p62 recognizes ubiquitinated cellular materials and incorporates them into the autophagic process via its chaperone-like function. As the LC3-II protein level is a marker of autophagy, the p62 protein level is frequently evaluated, particularly as a marker of the termination stage of autophagy. (Feng et al., 2014; Ichimura and Komatsu, 2010; Bitto et al., 2014).

Lysosomal markers are crucial in autophagy as they are used to identify autophagolysosomes, monitor their fusion with lysosomes, and thereby track autophagic flow. Lysosomal associated membrane protein-1 and -2 (LAMP-1 and LAMP-2) are lysosomal membrane integral glycoproteins that are frequently used as lysosomal markers (Eskelinen, 2006; Mizushima et al., 2010). The interaction between LAMP-1 and LC3 helps with the fusion of autophagosomes with lysosomes by recruiting lysosomal-associated membrane proteins to the autophagosome membrane. LAMP-1 and LC3 interaction is crucially evaluated to identify autophagosomes and autophagosome-lysosome fusion. (Yoshii and Mizushima, 2017; Mizushima et al., 2010; Pugsley, 2017;

Yim and Mizushima, 2020). As an addition to LAMP-1-LC3, several studies have shown that in autophagic machinery, LAMP-1 and p62 interact with each other for the degradation of ubiquitinated intracellular materials. LAMP-1-p62 interaction is one of the markers for monitoring autophagosome formation and tracking of autophagosome-lysosome fusion (Yoshii and Mizushima, 2017; Mizushima et al., 2010; Bjørkøy et al., 2006; Yim and Mizushima, 2020). Intra- or extracellular stressors or several disease conditions can lead to impaired autophagic flux which results in the accumulation of LC3 and p62 proteins as secondary autophagic substrates (Yoshii and Mizushima, 2017; Runwal et al., 2019).

1.7. Cathepsins and Autophagy

Cathepsins are acid hydrolase enzymes with diverse functions which are mostly localized and work in endo/lysosomal compartments. In addition to their role in the lysosome, cathepsins are also involved in cellular processes such as apoptosis, immune response, and energy metabolism by being present in the extracellular space and cytoplasm. As a lysosomal hydrolase enzyme, cathepsins have a role in the degradation of their several cellular substrates in the endo/lysosomal compartment and so they are involved in autophagic flux (Figure 1.4) (Yadati et al., 2020; Müller et al., 2012). For example, the initiation of autophagy, formation of autophagosome, and fusion of autophagosome and lysosome are not affected in the deficiency of Cathepsin L in mouse embryonic fibroblasts but the degradation of autophagosomal content is impaired (Dennemärker et al., 2010). Also, Cathepsin S deficiency causes increased autophagosome number (Yang et al., 2014).

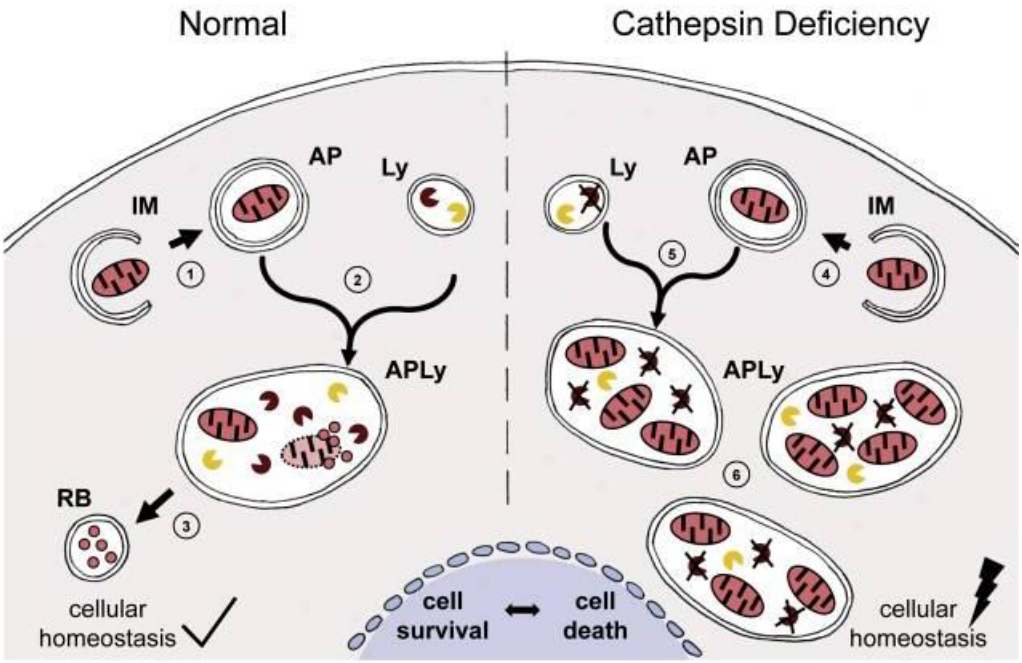

Figure 1.4: Role of cathepsins in macroautophagy. Dysfunctional, long-lived, or superfluous macromolecules or organelles are subjected to degradation via autophagy within the double-membrane vesicle, also known as isolation membrane (IM). Then, autophagosome (AP) formation is followed (1). AP fuses with the lysosome (Ly) to form autophagolysosome (APLy) (2), and cellular cargo is degraded with lysosomal enzymes. Residual body (RB) formation (3) after lysosomal degradation is limited in healthy cellular conditions. In cathepsin deficiency conditions, IM, AP, or APLy formation is not primarily affected (4,5). Lack of proteolytic activity of cathepsins results in non-degraded cellular cargos, an increased number of large APLy vesicles (6), and dysregulated cellular homeostasis caused by impaired autophagic flux (Source: Müller et al., 2012).

Cuervo and her colleagues have identified that lysosomal CathA has a regulatory role in chaperone-mediated autophagy (CMA). Serine carboxypeptidase CathA hydrolyzes the splice variant of LAMP2, Lamp2a, which is a rate-limiting factor of CMA. Cuervo's study has shown that an increased amount of Lamp2a in the lysosomal membrane caused by the reduced rate of Lamp2a degradation results in higher levels of CMA in Galactosialidosis patients fibroblasts and Galactosialidosis mouse model (*CathA*$^{-/-}$) tissues (Cuervo et al., 2003).

1.8. Aim of the Thesis Study

In this thesis study, the aim was to investigate the role of lysosomal Cathepsin A enzyme, without its catalytic activity, in autophagic flux. To achieve this aim, we have used fibroblast and neuroglia cell lines which were generated from 1-month-old catalytically inactive Cathepsin A mice ($CathA^{S190A}$) and their wild-type littermates. Previously, the accumulation and distribution of short bioactive peptides in the tissues of $CathA^{S190A}$ mice were demonstrated because of the lack of catalytic activity of lysosomal CathA. The effect of accumulated short bioactive peptides in $CathA^{S190A}$ mice on autophagic flux has been sub-aimed in this thesis study. Altogether, this thesis study helps us to understand whether the lysosomal Cathepsin A enzyme has a regulatory role in the regulation of autophagic flux *in vitro* through its serine carboxypeptidase catalytic activity.

CHAPTER 2

MATERIALS AND METHODS

2.1. Breeding of Mice

Catalytically inactive lysosomal Cathepsin A mouse model, $CathA^{S190A}$, which carries a point mutation by replacing serine amino acid with alanine in the active catalytic site was generated by Prof. Dr. Volkan Seyrantepe during post-doctoral studies (Seyrantepe et al. 2008). The homozygote point mutation carrying mouse was bred with C57BL/6 which is a wild-type mouse strain, to generate heterozygote male and female mice. As an F1 generation, generated male and female heterozygote mice ($CathA^{+/S190A}$) were bred with each other to generate homozygote colonies which are homozygote $CathA^{S190A/S190A}$ and $CathA^{+/+}$ control littermates. After the generation of homozygote $CathA^{S190A}$ and $CathA^{+/+}$ colonies, mutant and control colonies were purely interbred only. Breeding pairs from siblings were selected to reduce and minimize genetic variations among mice that could arise in subsequent generations.

2.2. Genotyping of Mice

Mice genotyping was done from the genomic DNA which was extracted from cut tail tissues of mice. The cut tails were incubated overnight within the 250 µl tissue lysis buffer (containing pH 7.6 1M Tris-Base (10 %), 0.2M Ethylenediamine Tetraacetic Acid (EDTA), sodium dodecyl sulfate (SDS, 20%) and 5M NaCl (4%)) and 6 µl Proteinase K solution (main stock was diluted to 25 µg/µl) in shaker incubator at 55°C and 70 rpm. On the following day, the samples were centrifuged for 10 minutes at 14000 rpm. After the centrifuge, obtained supernatants were taken into the new eppendorf tubes and 500 µl isopropanol (100%) was added also the new tubes. Precipitated DNA was collected and taken into the new eppendorf tubes which included 70% ethanol. Then, the eppendorf tubes were centrifuged at 14000 rpm for 1 minute and the supernatant was withdrawn from the eppendorf tubes and the eppendorf tubes were air dried to completely remove

the remaining 70% ethanol for 15 minutes. Precipitated DNA was incubated within the 100 µl ultra-pure water for 1 hour at 55°C for dissolving of the DNA. DNA concentrations were measured by using a Nanodrop spectrophotometer (ND-100).

Polymerase chain reaction (PCR) was set to identify $CathA^{S190A}$ and the wild-type control group using 100ng genomic DNA. In addition to genomic DNA; primers (50 pmol for forward and reverse), dNTPs (10 mM), Taq polymerase (1.5 units, Invitrogen), $MgCl_2$ (1.5 mM), Tris-HCl (10 mM) and KCl buffer (50 mM) including 10% DMSO were involved in the 50 µl PCR reaction mixture. Primers that are allele-specific for $CathA^{S190A}$ and $CathA^{+/+}$ were used (Table 2.1). PCR conditions were 1x cycle at 95°C for 30 seconds; 30x cycles at 95°C for 30 seconds, at 60°C for 45 seconds, at 72°C for 45 seconds; 1x cycle at 72°C for 5 minutes. After the PCR; to reveal the $CathA^{S190A}$ allele, an enzyme-cutting reaction was set up because the $CathA^{S190A}$ allele contains an enzyme recognition site for NdeI enzyme. 20 µl of the first PCR product, 20 units of NdeI (New England Biolabs) in 1X enzyme buffer were incubated for 3 hours.

Table 2.1: Primer sequences that were performed in genotyping

Gene	Primer	Sequence
$CathA^{S190A}$	ScreenF	GGTGGCGGAGAACAATTATG
	ScreenR	AACAGAAGTGGCACCCTGAC

2.3. Neuroglia Cell Line Generation

Neuroglia cells in the central nervous system (CNS) are composed of microglia cells, astrocyte cells, and oligodendrocyte cells (Aschner et al., 1999). Adult Brain Dissociation Kit (MACS Miltenyi Biotec, 130-107-677) and Adult Neuron Isolation Kit (MACS Miltenyi Biotec, 130-126-602) were used to isolate neuroglia cells from $CathA^{+/+}$ and $CathA^{S190A}$ mice. Enzyme A, Enzyme P, Buffer Z, Buffer Y, Debris Removal Solution (10X), Red Blood Cell Removal Solution, and Non-neuronal cell biotin antibody cocktail were provided within the Adult Brain Dissociation Kit and Adult Neuron Isolation Kit by the manufacturer. Additionally, gentleMACS™ Dissociator (Miltenyi Biotec, 130-093-235), gentleMACS™ C Tubes (Miltenyi Biotec, 130-096-334), MACS® SmartStrainers (70 µm, Miltenyi Biotec, 130-098-462), MACS Magnetic MultiStrand (130-042-303), MACS® BSA Stock Solution (Miltenyi Biotec, 130-091-

376) and 10X Dulbecco's Phosphate Buffered Saline (D-PBS, Biowest, X0520) were procured to isolate neuroglia cells. Dissociation of adult neural tissue, cell debris removal, red blood cell removal, and magnetic separation of neuron and non-neuron (neuroglia) using non-neuron specific antibody cocktail steps were followed during the isolation of neuroglia cells, respectively and all of these steps were done in Class II Laminar Cabin (Mars Safety Class 2, SCANLAF).

2.3.1. Dissociation of Adult Neural Tissue

40-days old *CathA*$^{+/+}$ and *CathA*^{S190A} mice were sacrificed using the cervical dislocation method and the whole brains of the mice were dissected into the cortex, thalamus, cerebellum, and hippocampus region. The cortex regions of the mouse brains were weighed as 100 mg. The cortex regions of mice brains were washed with cold D-PBS to completely remove blood from the cortex regions and the cortex regions were cut into smaller pieces using lancets. The brain particles were transferred to C tubes containing enzyme mix 1 which was a mixture of 50 µl Enzyme P and 1900 µl Buffer Z. C tubes were placed on the Dissociator and the program "m_brain_01" registered on the Dissociator was run. C tubes were then incubated at 37°C for 15 minutes in an incubator. C tubes were again placed on the Dissociator and the program "m_brain_02" registered on the Dissociator was run. After the second program on the Dissociator, enzyme mix 2 which was the mixture of 10 µl Enzyme A and 20 µl Buffer Y, was added to each C tube, and C tubes were incubated at 37°C for 15 minutes in an incubator. After the incubation, C tubes were centrifuged at 800 rpm for 1 minute to collect the samples at the bottom. SmartStrainers (70 µm) were placed for each brain on 50 ml falcon tubes and SmartStrainers were moistened using 3 ml of cold D-PBS. Centrifuged brain tissues were mixed by pipetting and they were taken from a C tube and applied to the SmartStrainers. 10 ml of cold D-PBS was put into the C tubes to collect all homogenized brain tissue, C tubes were shaken and it was applied onto the SmartStrainers. After the liquid phase completely passed through the strainer, the cell suspensions collected in a 50 ml falcon tube were centrifuged at 300 xG for 10 minutes at 4°C, and supernatants were completely removed from the falcon tubes. The cell debris removal step was proceeded using cell pellets.

2.3.2. Cell Debris Removal

Cell pellets were gently resuspended with 1550 µl cold D-PBS, cell suspensions were transferred to 15 ml falcon tubes and 450 µl cold Debris Removal Solution also was added to 15 ml falcon tubes. Cell suspension and cold Debris Removal Solution were mixed gently by pipetting up and down. 450 µl cold D-PBS was also overlayed gently on the mixture. Falcon tubes were centrifuged at 3000xG for 10 minutes at 4°C with full acceleration and brake. Three phases had formed after centrifugation and the top two phases are completely removed from the falcon tubes. The bottom phase containing falcon tubes was filled up with 15 ml with cold D-PBS and falcon tubes were inverted 4-5 times very carefully. Then, the falcon tubes were centrifuged at 1000 xG for 10 minutes at 4°C with full acceleration and brake. Supernatants were completely discarded from the falcon tubes. The procedure was followed with the Red Blood Cell Removal step.

2.3.3. Red Blood Cell Removal

1X Red Blood Cell Removal Solution was prepared by diluting the 10X Red Blood Cell Removal Solution with double-distilled water (ddH_2O) and cell pellets in the 15 ml falcon tubes were resuspended with 500 µl 1X Red Blood Cell Removal Solution and cell suspension were incubated at 4°C for 10 minutes. PB buffer was prepared by mixing MACS® BSA Stock Solution with cold D-PBS in a 1:20 ratio. After incubation, 5 ml of PB buffer was added to each falcon tube, falcon tubes were centrifuged at 300 xG for 10 minutes at 4°C, and supernatants were completely aspirated after the centrifuge.

2.3.4. Magnetic Separation of Neuron and Non-neuron Cells

The remaining cell pellets were resuspended with PB buffer. 20 µl Non-neuronal cell biotin antibody cocktail was added onto the resuspended cell pellets, then the samples were incubated at 4°C for 10 minutes. PB buffer was added so that the total volume was 500 µl. After this stage, the magnetic separation section was followed. LS columns were placed in a magnetic field by MACS Magnetic MultiStrand (magnetic separator) and washed with 3 ml of PB buffer. Cell mixtures were loaded onto the columns and the

flowing solutions were collected. The columns were washed with 2x1 ml of PB buffer and combined with the eluted solution from the previous step. The columns were separated from the magnetic separator and placed under 15 ml of the falcon, and glia cells were collected with a syringe by adding 3 ml of PB buffer. Supernatants were removed after the collected samples were centrifuged at 800 rpm for 10 minutes. Remaining cell pellets were resuspended with 100 µl Dublecco's Modified Eagle Medium (DMEM, Gibco, 12491015) containing 10% Fetal Bovine Serum (FBS, Gibco, A4766801) and 1% Penicillin-Streptomycin (Pen-Strep, Gibco, 15140122). Finally, the resuspended neuroglia cells were seeded as primary cells into a T25 cell culture flask (Greiner, 690160) containing 5 ml of DMEM (10% FBS, 1% Pen-Strep). Resuspended cells were incubated for 2 days at Thermo Scientific™ Midi 40 CO_2 Incubator (ThermoFisher Scientific, 3403) with the conditions of 5% CO_2, 37°C and 75% humidity to wait for the cells to recover from the stress condition and show their morphology. After 2 days, the cells were immortalized by following the steps which are explained in detail in section 2.5.

2.4. Fibroblast Cell Line Generation

40-days old *CathA*$^{+/+}$ and *CathA*^{S190A} mice which were used in neuroglia isolation were used to establish fibroblast cell lines. Thus, both fibroblast and neuroglia cell lines were established from the same mice and two isolation protocols were applied simultaneously. After the mice were killed with cervical dislocation, the skin sample was first cleaned with 70% alcohol in rats whose chest hair was shaved. A 1 cm^2 biopsy sample was taken from the shaved skin surface and the biopsy sample was cut into small pieces using a scalpel. Well-shredded mouse skin pieces were placed in a T25 cell flask containing 5 ml of DMEM (10% FBS, 1% Pen-Strep), and fibroblast cells were waited to adhere to the flask surface by showing morphology for 2 days. At the end of 2 days, the skin pieces were completely removed from the T25 cell flask, and the cells were gently washed with 1X PBS. The cells were immortalized by following the steps which are explained in detail in section 2.5.

2.5. Immortalization of Neuroglia and Fibroblast Cells

Immortalization of primary cells is one of the most preferred experimental tools because cells derived from animal or human tissues have a limited ability to divide and therefore have a limited number of passages before entering the senescence and senescence-related death stage. Previous studies, immortalized cells; demonstrate that primary cells can maintain their shape, properties, and function and can replace primary cells to provide suitable and reliable experimental materials for basic scientific research, clinical treatments, bioengineering pharmaceuticals, and vaccine studies (Guo et al., 2022).

The packaging cell line, named as PA317 LXSN 16E6E7 (ATCC, CRL2203), was used for the immortalization of primary $CathA^{+/+}$ and $CathA^{S190A}$ fibroblast and neuroglia cells. This cell line was obtained by introducing a retrovirus vector, pLXSN16E6E7, into the Psi-2 ecotrophic cell line. Packaging cells containing the vector were grown at a concentration of 50-75% in antibiotic-free media. The culture medium was collected from these cells and passed through a 0.45 μm filter and diluted at the suggested ratio by the manufacturer. Then, 8 μg/ml polybrene (Sigma-Aldrich, TR-1003) was added to the final. The virus/polybrene solution was added to primary fibroblast and neuroglia cells obtained from mice and incubated for 2 hours at 37°C. Then, the polybrene was added to the DMEM solution at a final 4 μg/ml and incubated for another 5 hours. Cells were seeded at various dilutions and selected for 10 days by adding geneticin (Gibco, 10131027) to DMEM (10% FBS, 1% Pen-Strep).

2.6. Cell Culture Treatments

Immortalized $CathA^{+/+}$ and $CathA^{S190A}$ fibroblast and neuroglia cells were grown in an incubator at 37°C, 5% CO2, and 75% humidity. DMEM (10% FBS, 1% Pen-Strep) was removed during the passage, and after the cells were washed with 1X PBS, 1ml of 0.25% (w/v) trypsin-0.53mM EDTA (ThermoFisher Scientific, 25200056) solution was added to them and incubated at 37°C for about 5 minutes. The cells detached from the surface were centrifuged at 800 rpm for 5 minutes by adding 3 ml of DMEM (10% FBS, 1% Pen-Strep) on them. Cells were diluted at certain ratios and continued to be grown in

T75 cell culture flasks (Greiner, 658170) adding 10-12 ml of DMEM (10% FBS, 1% Pen-Strep) in an incubator at 37°C, 5% CO2, and 75% humidity. During culture, DMEM (10% FBS, 1% Pen-Strep), was renewed every 2-3 days. After the cells reached 70% confluency, they were grown in 100 mm^2 cell culture dishes (Greiner Cellstar®, 664160) under different treatment conditions, separately for each cell type and each genotype for molecular biological analysis. The treatment conditions to the cells were as follows: **(i)** non-treated condition **(None)**, **(ii)** Rapamycin treatment for 1 hour with a final concentration of 200 nM **(Rapamycin)**, **(iii)** incubation with starvation medium EBSS for 2 hours **(Starvation)** and **(iv)** During the incubation with EBSS medium for 2 hours, Rapamycin is added to the EBSS medium at the end of the first 1 hour, with a final concentration of 200 nM **(Starvation-Rapamycin)**. For rapamycin treatment, 1M stock Rapamycin (Enzo Life Sciences, BML-A275-0005) solution dissolved in 100% DMSO (ThermoFisher Scientific, 85190) was added into DMEM or EBSS medium at a ratio of 1:5000 to 200 nM.

2.7. Real-Time PCR (RT-PCR)

Protocol for RT-PCR was performed by following the isolation of RNA, synthesis of cDNA, and RT-PCR steps, respectively.

2.7.1. Isolation of RNA

1 mL GeneZol (GeneAid) was added into the falcon tubes which separately contained none-treated, rapamycin-treated, starvation medium incubated, and rapamycin-treated after starvation medium incubated $CathA^{+/+}$ and $CathA^{S190A}$ fibroblast and neuroglia cell pellets harvested from 100 mm^2 flasks, and incubated for 5 minutes at room temperature. At the end of the incubation, samples were transferred into the 1.5 mL eppendorf tubes, 200 µl chloroform was added into each eppendorf tube, the samples containing eppendorf tubes were shaken gently for 3-4 times and samples were incubated at room temperature for 2 minutes. The samples were centrifuged at 15000 rpm for 15 minutes at +4°C for phase separation. After the centrifuge was completed, RNA containing the colorless upper phase was taken into new 1.5 mL eppendorf tubes

containing 500 µl isopropanol for the precipitation of RNA, mixture in the new eppendorf tubes was pipetted several times, incubated for 10 minutes at room temperature and the samples were centrifuged at 15000 rpm for 10 minutes at +4°C. After the centrifugation, the supernatant was completely removed and 1 ml 70% ethanol was put on the remaining pellets for the washing. The eppendorf tubes were carefully and briefly vortexed and centrifuged at 7500 rpm for 5 minutes at +4°C. Alcoholic supernatant was discarded and RNA pellet containing eppendorfs were air-dried for 5-10 minutes at 55°C. For the resuspension of the RNA pellets, 50-100 µl RNase-free water was put into the eppendorf tubes and the eppendorf tubes were incubated in water-bath at 55°C for 15 minutes to completely dissolve RNA. RNA concentrations of the samples were measured in NanoDrop Spectrophotometer (ND-1000).

2.7.2. Synthesis of cDNA

RNA samples were converted to cDNAs using a cDNA Synthesis Kit (Abcam). The reaction mixture was prepared so that 50 ng/µl of cDNA was obtained from each sample at the end of the reaction according to the manufacturer's instructions. Novo RTase (200 unit/µl), 5X RT Buffer, dNTPs (10mM), random primers (10µM), and calculated volume of RNA and water depending on the concentration of RNAs for each sample were included in the reaction mixture with a total volume of 20 µl. cDNA converting reaction conditions were as follows: 1X cycle at 25°C for 10 minutes, 1X cycle at 55°C for 15 minutes and 1X cycle at 72°C for 5 minutes.

To check whether the RNAs were successfully converted to cDNA, normal PCR for GAPDH was set up in each of the samples from the cDNA conversion reaction. PCR mixture for the GAPDH gene was as follows: 50 ng of cDNA, forward and reverse primers for GAPDH (0.8 mM), dNTP mix (10 mM), 1X buffer including $MgCl_2$ and 2 units of Invitrogen Taq DNA Polymerase (ThermoFisher) with a total volume of 25 µl of reaction. GAPDH PCR reaction was run in the conditions that 1X cycle at 95°C for 2 minutes; 30X cycles at 95°C for 20 seconds, at 65°C for 15 seconds, at 72°C for 20 seconds; 1X cycle at 72°C for 3 minutes. After the PCR, the sample's reaction products were subjected to agarose gel electrophoresis in 1% agarose gel at 95 volts for 35 minutes.

2.7.3. RT-PCR

Roche LightCycler® 96 System with Roche LightCycler 480 SYBR Green I Master Mix were used for calculation and measurement of relative expression levels of genes which were listed in Table 2.2 with their product length sizes. Forward and reverse primers (0.4 μM), 1X Roche LightCycler 480 SYBR Green I Master Mix, and 75 ng cDNA were added to the reaction tube to measure each gene's relative expression pattern with a total volume of 20 μl of reaction. RT-PCR reaction conditions were as follows: 1X cycle at 95°C for 10 minutes; 45X cycles at 95°C for 20 seconds, at 58°C for 20 seconds, at 72°C for 20 seconds. This reaction was repeated 3 times for each sample and the average level of gene expression in each sample was measured by averaging the 3 results. These gene expression levels were normalized to the GAPDH gene, which is a housekeeping gene, and so the gene expression ratio of each gene was obtained. Statistical analyses were done using the Two-way *ANOVA* method on GraphPad Prism.

Table 2.2: Forward and reverse primers of autophagy-marker genes

Gene	**Primer Sequences**	**Product Length (bp)**
Beclin-1	F:5'-GAGGAGCAGTGGACAAAAGC-3' R: 5'-CAAACATCCCCTAAGGAGCA-3'	112 bp
ATG9	F:5'-GTGCTTATTGCCCTCACCAT-3', R: 5'-GGCATGTAGTGGATGTGTGC-3'	179 bp
ATG7	F: 5'-GTCGTCTTCCTATTGATGGACACC-3' R: 5'-CAAAGCAGCATTGATGACCAGC-3'	93 bp
p62	F: 5'-TGTGGAACATGGAGGGAAGAG-3' R: 5'-TGTGCCTGTGCTGGAACTTTC-3'	67 bp
LAMP2	F: 5'-TAACATCAACCCTGCCACAA-3' R: 5'-AAGCTGAGCCATTAGCCAAA-3'	176 bp
GAPDH	F:5'-CCCCTTCATTGACCTCAACTAC-3' R:5'-ATGCATTGCTGACAATCTTGAG-3'	347 bp

2.8. Western Blot

Isolation of proteins, Bradford assay, and SDS-Polyacrylamide Gel Electrophoresis (SDS-PAGE) steps were followed respectively for the Western Blot method.

2.8.1. Isolation of Proteins

To obtain protein lysates from fibroblast and neuroglia cells treated in the above-mentioned conditions, cell groups were homogenized in 100 µl RIPA buffer (TritonX100 (1%), NaCl (150 mM), Glycerol (10%), HEPES (50 mM), TrisBase (50 mM), PMSF (1%, Sigma-Aldrich) and Protease inhibitor cocktail (1%, Sigma-Aldrich)), a protein lysis solution, using a homogenizer. After the cell lysates were homogenized in RIPA solution, they were kept on ice for 1 hour by vortexing every 10 minutes and centrifuged at 14000 rpm for 15 minutes at 0°C after 1 hour. After centrifugation, the supernatants containing the proteins were transferred to new eppendorf tubes.

2.8.2. Bradford Assay

Bradford Assay was performed to determine the concentration of isolated proteins from cell samples in µg/µl. The protein samples which were isolated from treated and untreated fibroblast and neuroglia cell lines, were diluted in 1/100 ratio (4 µl protein sample+396 µl dH_2O). Diluted protein samples were put into the 96-well plate as 50 µl, together with the BSA solutions prepared at different concentrations (100, 80, 40, 20, and 10 ng/µl), in order to obtain a standard curve. Then, 200 µl of Bradford Reagent (BioRad) was added to the protein samples. After the samples were incubated with Bradford Reagent for 10 minutes, absorbance values were measured at 595 nm wavelength in Microplate Reader (BioRad). A standard curve graph was drawn using the absorbance values of diluted BSA solutions at different concentrations, and the concentration of each protein sample was calculated using the equation obtained from this standard curve graph.

Finally, loading protein samples were prepared such that the amount of protein in each sample was 20 µg by adding an appropriate amount of water and in 1/4 ratio of loading dye containing glycerol (40%), Tris-HCl (ph 6.8, 240 mM), SDS (8%), Bromophenol blue (0.04%) and ß-mercaptoethanol (5%).

2.8.3. SDS-PAGE

Resolving gel (10%) was prepared that as shown in Table 2.3, and poured into glasses that were clamped between plastic frames. 2 ml of isopropanol was added on top of the resolving gel in order to prevent air gaps that may occur in the resolving gel. After the resolving gel polymerized, the isopropanol was removed from the glasses, and the stacking gel prepared as indicated in Table 2.3 was poured onto the resolving gel. In addition, with the pouring of the stacking gel, suitable combs were placed between the glasses to form the wells to be loaded. After the stacking gel frozen and polymerized, the inserted comb was removed from between the glasses, and the glass was separated from the plastic frames and placed in the tank containing the running buffer containing TrisBase (0.25 M), Glycine (1.92 M) and SDS (1%). Previously prepared loading protein samples were boiled at 95°C for 10 minutes and loaded into the wells with the protein ladder (BioRad). Loaded protein samples were run at 120V until switching from stacking gel to resolving gel. After the protein samples were transferred to the stacking gel, they were separated by running for approximately 90 minutes. Proteins run in SDS-PAGE were transferred to the nitrocellulose membrane (BioRad) in the transfer chamber within the transfer sandwich. Proteins in the transfer cassette filled with pH 9.2 transfer buffer which consisted of TrisBase (48 mM), glycine (39 mM), and methanol (20%) were transferred at 250 mA for 75 minutes. After the completion of the transfer, the membranes (blots) were incubated in the blocking solution (milk powder (5%) dissolved in 1X PBS-T (0.005% Tween20)) for 1 hour at room temperature for blocking. After blocking, the blots were washed 3 times for 5 minutes in 1X PBS.

The washed blots were then incubated at +4°C overnight with diluted primary antibodies which were anti-LC3 (1:10000, Cell Signaling Technology, 2775S), anti-SQSTM1/p62 (1:10000, Cell Signaling Technology, 16177) and anti-ß-actin (1:10000, Cell Signaling Technology, 13E5), dissolved in the red solution (Phenol Red (0.04%),

NaAzide (0.02%), BSA (5%) in pH 7.5 1X PBS-T). The washed blots were then incubated at +4°C overnight with diluted primary antibodies in the red solution (Phenol Red (0.04%), NaAzide (0.02%), BSA (5%) in pH 7.5 1X PBS-T) which were anti-LC3 (1:2000, Cell Signaling Technology, 2775S), anti-SQSTM1/p62 (1:2000, Cell Signaling Technology, 16177) and anti-ß-actin (1:10000, Cell Signaling Technology, 13E5). The next day, overnight incubated blots were washed 3 times for 5 minutes in 1X PBS. Washing was followed by incubation of the blots for 1 hour at room temperature with the HRP-conjugated secondary antibody (Jackson ImmunoResearch Lab)secondary antibodies dissolved in the blocking solution used in the blocking process. After the secondary antibody incubation, the blots were washed 3 times for 5 minutes and the proteins were visualized using LuminataTM Forte Western HRP Substrate (Millipore) on a computational imaging system (Fusion SL, Vilber Lourmat). This Western Blot protocol was repeated 3 times for each cell line's treated and non-treated samples and the average level of proteins in each sample was measured by averaging the 3 results. LC3 and p62 protein levels were normalized to ß-actin protein level which is an internal loading control. Statistical analyses were done using the Two-way ANOVA method on GraphPad Prism.

Table 2.3: Stacking and resolving gel ingredients for SDS-PAGE

5% Stacking Gel	**10% Resolving Gel**
3.5 ml dH_2O	5 ml dH_2O
1.5 ml pH 6.8, 1M Tris-HCl (Upper Buffer)	3 ml pH 8.8, 1M Tris-HCl (Lower Buffer)
1 ml 30% Acrylamide-Bis (BioRad)	4 ml 30% Acrylamide-Bis (BioRad)
60 µl Ammonium persulfate	60 µl Ammonium persulfate
60 µl SDS	60 µl SDS
6 µl Tetramethylethylenediamine	6 µl Tetramethylethylenediamine

2.9. Immunocytochemistry (ICC)

Immunocytochemistry (ICC) was performed for co-localize displaying of autophagic flux in treated and untreated fibroblast and neuroglia cells together with LC3 and p62, which are proteins involved in autophagic machinery, and LAMP1 protein, which is a lysosome marker. Fibroblast and neuroglia cells were seeded on a 24-well plate on circular slides and treated under the above-mentioned conditions after appropriate confluency. After the treatment times of the cells were completed, the medium was removed from the wells, and the cells were washed 3 times for 5 minutes with 1X PBS. Rinsed cells were incubated with 500 µl, paraformaldehyde (PFA, 4%, PFA dissolved in 1X PBS) for 1 hour for fixation. After fixation, cells were washed 5 times for 5 minutes with 1X PBS to completely remove PFA. After that, cells were incubated for 30 minutes with 500 µl TritonX100 (0.5%, TritonX100 dissolved in 1X PBS) for permeabilization. Cells were then incubated with 500 µl blocking solution (Goat Serum (10%), BSA (4%), TritonX100 (0.003%), glycine (0.3 M) dissolved in 1X PBS) for 1 hour at room temperature to block non-specific binding. After blocking solution incubation, cells were incubated overnight at 4°C with primary antibody solutions involving blocking solution which were anti-LC3 (1:200, Cell Signaling Technology, 2775S)/anti-LAMP1 (1:500, Abcam, ab24170) and anti-SQSTM1/p62 (1:200, Cell Signaling Technology, 16177)/ anti-LAMP1 (1:500, Abcam, ab24170). Cells were washed 3 times for 5 minutes with 1X PBS the next day. Washing steps were followed by incubation of the cells for 1 hour at room temperature with secondary antibodies (ab175476, Alexa Fluor®-568 and ab150077 Alexa Fluor®-488) involving blocking solution, and later on, cells were washed 3 times for 5 minutes with 1X PBS. The slides with treated and non-treated fibroblast and neuroglia cells were mounted with Fluoroshield mounting medium DAPI (Abcam). Cell images were obtained using a fluorescent microscope (Olympus BX53) under the appropriate wavelength of each protein and co-localization analysis of green and red fluorescences were processed using ImageJ. Statistical analyzes were performed using the Two-way ANOVA method in terms of "protein intensity/cell" by dividing the fluorescent green and red fluorescence by the number of cells in the image.

CHAPTER 3

RESULTS

3.1. Genotyping of Mice

PCR was performed to detect wild-type and knock-in mutant alleles. Wild-type ($CathA^{+/+}$), knock-in mutant ($CathA^{S190A/S190A}$), and heterozygote ($CathA^{+/S190A}$) mice were genotyped depending on the amplified PCR products.

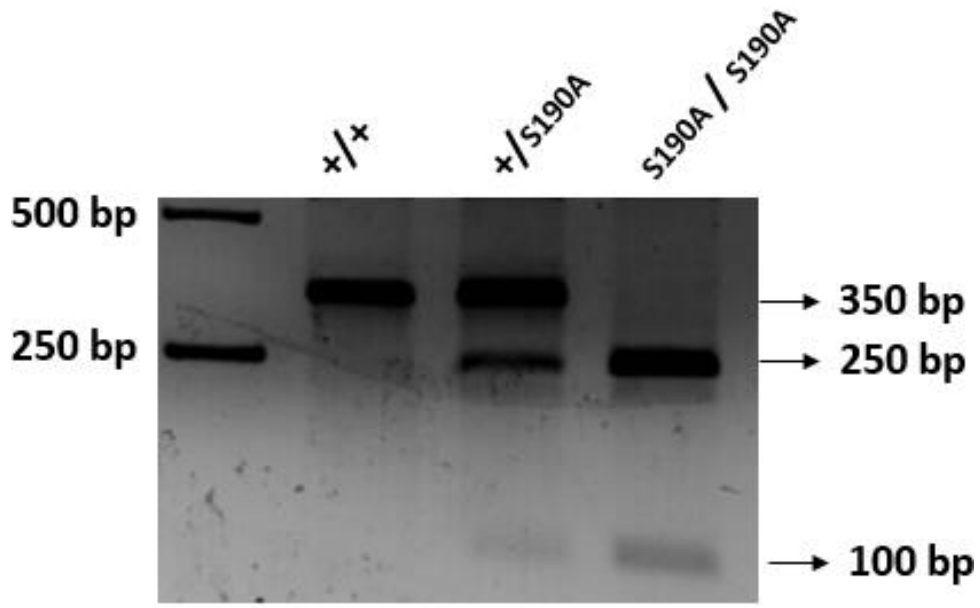

Figure 3.1. AGE image of PCR amplifications of *Ctsa* gene which was *NdeI* digested. ScreenF and ScreenR primers generated a 350-bp single fragment in $CathA^{+/+}$ mice; 350-,250- and 100-bp fragments in heterozygous $CathA^{+/S190A}$ mice; 250- and 100-bp fragments in homozygous $CathA^{S190A/S190A}$ mice.

3.2. Autophagic Machinery Analysis

To investigate whether there is an alteration in autophagic machinery and flux in fibroblast and neuroglia cells of catalytically inactive knock-in CathA mouse model, $CathA^{S190A}$, through gene and protein expression analysis were done. RT-PCR, Western

Blot, and Immunocytochemistry methods were performed to analyze autophagic flux with autophagy markers which are *Beclin-1*, *ATG9*, *ATG7*, *p62*, and *LAMP2* in gene expression and LC3, p62, and LAMP1 in protein expression.

3.2.1. RT-PCR

Quantitative RT-PCR was performed to see the alterations in gene expression levels of autophagic marker genes. *Beclin-1*, *ATG9*, *ATG7*, *p62*, and *LAMP2* relative gene expression levels were measured and analyzed in neuroglia and fibroblast cells of $CathA^{+/+}$ and $CathA^{S190A}$ mice

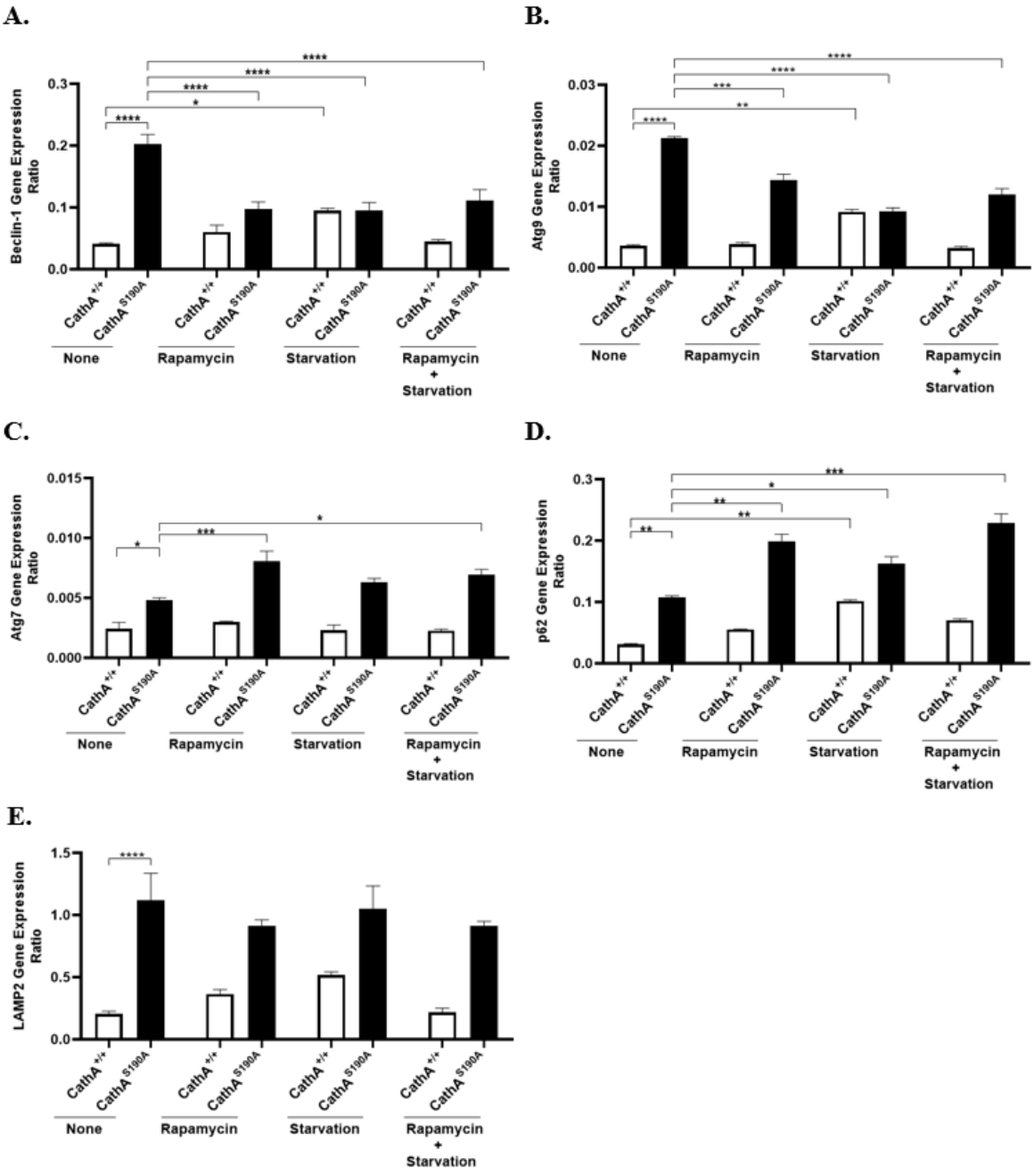

Figure 3.2. Relative gene expression ratios of autophagy marker genes of *CathA*$^{+/+}$ and *CathA*^{S190A} mice derived neuroglia cells in non-treated (none) and autophagy-inducing treatment conditions (Rapamycin, Starvation, and Rapamycin+Starvation). Gene expression levels of *Beclin-1* **(A)**, *Atg9* **(B)**, *Atg7* **(C)**, *p62* **(D),** and *LAMP2* **(E)** were normalized to the *GAPDH* gene. (n=3;*p<0,05,**p<0,01,***p<0,001,****p<0,0001) Expression ratios were calculated by ΔCT method and 2-way-ANOVA analysis was used to determine p-values via GraphPad Prism.

Beclin-1 gene expression level was significantly increased in non-treated (None) *CathA*^{S190A} neuroglia cells compared to non-treated (None) *CathA*$^{+/+}$ neuroglia cells. *Beclin-1* expression level of *CathA*$^{+/+}$ neuroglia cells significantly increased after the Starvation condition compared to non-treated (None) *CathA*$^{+/+}$ neuroglia cells, while no significant change in *Beclin-1* expression level was detected in Rapamycin and Rapamycin+Starvation conditions. On the other hand, all the autophagy-inducing conditions which were Rapamycin, Starvation, and Rapamycin+Starvation, led to a significant increase in *Beclin-1* expression level of *CathA*^{S190A} neuroglia cells compared to non-treated (none) *CathA*^{S190A} neuroglia cells (Figure 3.2.A).

In the perspective of *Atg9* gene expression level, a significant increase was seen in *CathA*^{S190A} neuroglia cells, compared to *CathA*$^{+/+}$ neuroglia cells in non-treated (None) condition. Among the autophagy-inducing treatment conditions, only the Starvation condition resulted in a statistically significant increase in *Atg9* expression in *CathA*$^{+/+}$ neuroglia cells, whereas all autophagy-inducing treatment conditions which were Rapamycin, Starvation, and Rapamycin+Starvation, resulted in a significant decrease in *Atg9* expression in *CathA*^{S190A} neuroglia cells (Figure 3.2.B).

Atg7 gene expression level was also significantly increased in non-treated (None) *CathA*^{S190A} neuroglia cells compared to non-treated (None) *CathA*$^{+/+}$ neuroglia cells. No significant change in the *Atg7* gene expression level of *CathA*$^{+/+}$ neuroglia cells was seen in autophagy-inducing treatment conditions which were Rapamycin, Starvation, and Rapamycin+Starvation. In *CathA*^{S190A} neuroglia cells, Rapamycin and Rapamycin+Starvtion conditions significantly increased the *Atg7* gene expression level compared to non-treated (None) *CathA*^{S190A} neuroglia cells, while no significant difference was detected in the *Atg7* gene expression level in Starvation condition. (Figure 3.2.C).

p62 gene expression level was significantly high in non-treated (None) *CathA*^{S190A} neuroglia cells, compared to non-treated (None) *CathA*$^{+/+}$ neuroglia cells. When autophagy-inducing treatment conditions were applied to *CathA*$^{+/+}$ neuroglia cells, the *p62* gene expression level was significantly increased only in the Starvation condition, while it showed insignificant increases in the other treatment conditions which were Rapamycin and Rapamycin+Starvation, compared to their non-treated (None) condition. On the other hand, autophagy-inducing conditions were applied to the catalytically inactive *CathA*^{S190A} neuroglia cells, it was determined that the *p62* gene expression level increased in all conditions compared to the untreated conditions. (Figure 3.2.D).

LAMP2 gene expression level was significantly increased in non-treated (None) *CathA*^{S190A} neuroglia cells compared to non-treated (None) *CathA*$^{+/+}$ neuroglia cells. None of the autophagy-inducing conditions resulted in a statistically significant change in the gene expression level of *LAMP2* in *CathA*$^{+/+}$ and *CathA*^{S190A} neuroglia cells. Nevertheless, the gene expression level of *LAMP2* slightly increased in Rapamycin and Starvation conditions in *CathA*$^{+/+}$ neuroglia cells and slightly decreased in Rapamycin and Rapamycin+Starvation conditions in *CathA*^{S190A} neuroglia cells (Figure 3.2.E).

To summarize in general, according to the quantitative RT-PCR results we have done; It was found that the gene expression levels of the autophagy-related genes *Beclin-1*, *Atg9*, *Atg7*, *p62*, and *LAMP2* were significantly increased in non-treated *CathA*^{S190A} neuroglia cells compared to non-treated *CathA*$^{+/+}$ neuroglia cells. Subsequently, various alterations were seen in *CathA*^{S190A} and *CathA*$^{+/+}$ neuroglia cells after both cell types were treated with autophagy-inducing conditions which were Rapamycin, Starvation, and Rapamycin+Starvation (Figure 3.2).

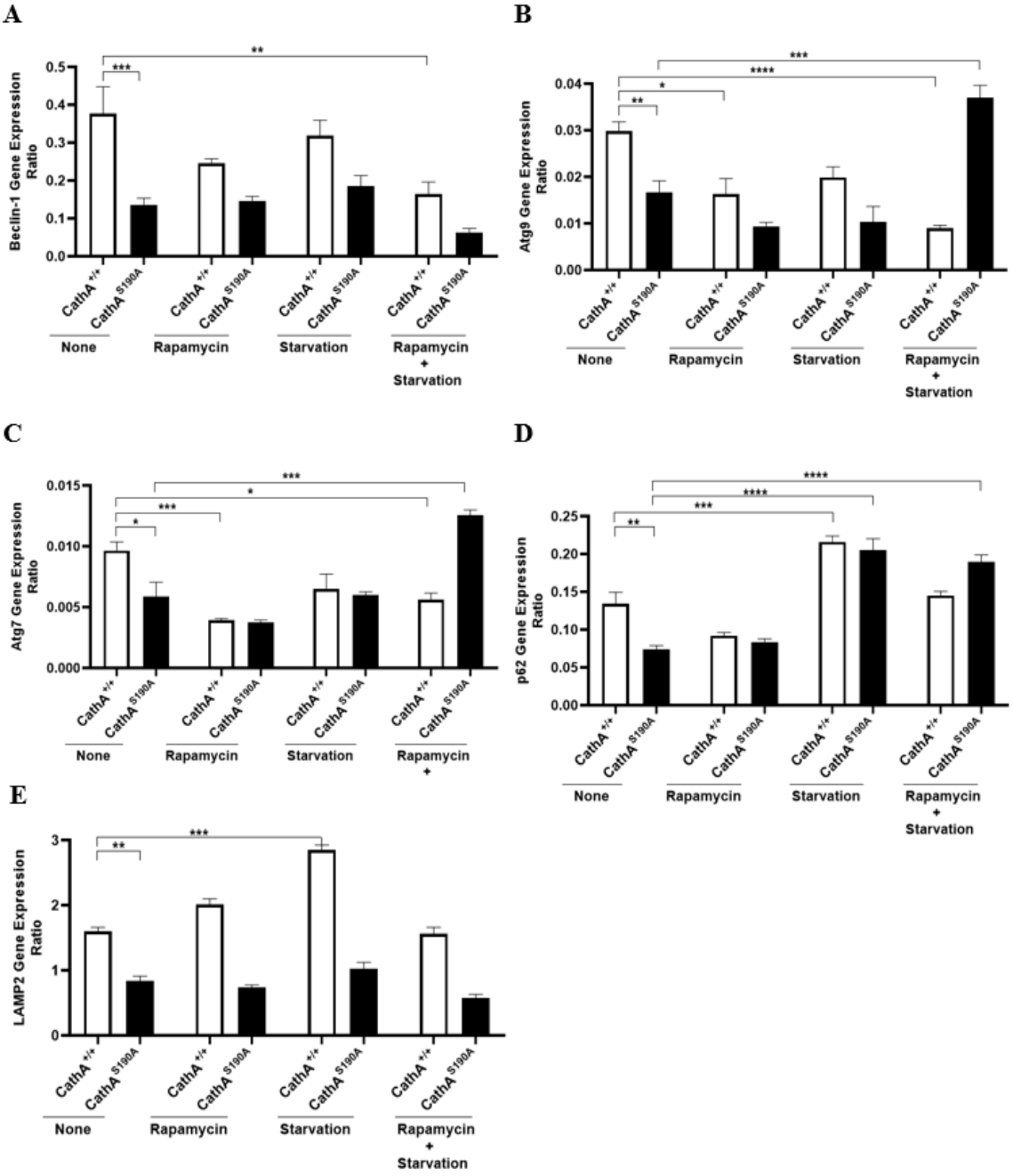

Figure 3.2. Relative gene expression ratios of autophagy marker genes of *CathA*$^{+/+}$ and *CathA*^{S190A} mice derived fibroblast cells in non-treated (none) and autophagy-inducing treatment conditions (Rapamycin, Starvation, and Rapamycin+Starvation). Gene expression levels of *Beclin-1* **(A)**, *Atg9* **(B)**, *Atg7* **(C)**, *p62* **(D),** and *LAMP2* **(E)** were normalized to the *GAPDH* gene. (n=3;*p<0,05,**p<0,01,***p<0,001,****p<0,0001) Expression ratios were calculated by ΔCT method and 2-way-ANOVA analysis was used to determine p-values via GraphPad Prism.

Non-treated (none) *CathA*$^{+/+}$ mouse-derived fibroblast cells' expression level of the *Beclin-1* gene was significantly increased compared to *CathA*^{S190A} mouse-derived fibroblast cells' *Beclin-1* gene expression level. The gene expression level of *Beclin-1* in *CathA*$^{+/+}$ fibroblast cells decreased significantly only in Rapamycin+Starvation condition among autophagy-inducing conditions compared to non-treated (none) condition, while a statistically insignificant decrease was determined in Rapamycin and Starvation conditions. In catalytically inactive *CathA*^{S190A} fibroblast cells, while the *Beclin-1* gene expression level did not significantly change after any autophagy-inducing treatment compared to the non-treated (None) condition, there was an insignificant increase in the Starvation condition and an insignificant decrease in the Rapamycin+Starvation condition (Figure 3.3.A).

The expression level of the *Atg9* gene was significantly increased in non-treated (none) *CathA*$^{+/+}$ fibroblast cells compared to non-treated (none) *CathA*^{S190A} fibroblast cells. Rapamycin and Rapamycin+Starvation treatments led to a significant decrease in the gene expression level of *Atg9* in *CathA*$^{+/+}$ fibroblast cells compared to non-treated (None) condition and in the meantime, a slight but not statistically significant decrease in the gene expression level of *Atg9* in *CathA*$^{+/+}$ fibroblast cells after Starvation treatments was seen. On the other hand, the *Atg9* gene expression level of *CathA*^{S190A} fibroblast cells significantly increased with Rapamycin+Starvation treatment and the expression level of *Atg9* slightly but insignificantly decreased after Rapamycin and Starvation treatment conditions (Figure 3.3.B).

Atg7 gene expression level of non-treated (None) *CathA*$^{+/+}$ fibroblast cells was significantly high compared to non-treated (None) *CathA*^{S190A} fibroblast cells. Rapamycin and Rapamycin+Starvation autophagy-inducing treatments resulted in a statistically significant decrease in the expression level of the *Atg7* gene in *CathA*$^{+/+}$ fibroblast cells compared to the non-treated (none) condition, while the Starvation treatment condition resulted in slight but not significant decrease of the expression level of *Atg7* gene in *CathA*$^{+/+}$ fibroblast cells compared to non-treated (none) condition. The gene expression level of *Atg7* of *CathA*^{S190A} fibroblast cells significantly changed by increasing only after Rapamycin treatment condition among the autophagy-inducing conditions compared to non-treated *CathA*^{S190A} fibroblast cells (Figure 3.3.C).

In non-treated (none) *CathA*$^{+/+}$ fibroblast cells, compared to non-treated (None) catalytically inactive *CathA*^{S190A} fibroblast cells, the gene expression level of *p62* was significantly increased. Starvation treatment led to statistically significant increased *p62*

gene expression level in *CathA*$^{+/+}$ fibroblast cells compared to non-treated (None) condition; Rapamycin and Rapamycin+Starvation conditions did not significantly change the gene expression level of *p62* in CathA$^{+/+}$ fibroblast cells. The *p62* gene expression level in *CathA*^{S190A} fibroblast cells was not changed by Rapamycin treatment compared to the non-treated condition but increased significantly under the Starvation and Rapamycin+Starvation treatment conditions (Figure 3.3.D).

The expression level of the *LAMP2* gene in non-treated (None) *CathA*$^{+/+}$ fibroblast cells was also significantly high compared to non-treated (None) *CathA*^{S190A} fibroblast cells. Only the Starvation treatment condition significantly increased the gene expression level of *LAMP2* in *CathA*$^{+/+}$ fibroblast cells compared to the non-treated (None) condition. None of the autophagy-inducing treatment conditions which were Rapamycin, Starvation, and Rapamycin+Starvation, did not affect significantly the expression level of the *LAMP2* gene in *CathA*^{S190A} fibroblast cells compared to the non-treated (None) condition (Figure 3.3.E).

In summary, according to quantitative RT-PCR results and analyses; It was determined that the expression levels of *Beclin-1*, *Atg9*, *Atg7*, *p62*, and *LAMP2* genes, which are known to be genes associated with autophagic flux, were significantly higher in non-treated *CathA*$^{+/+}$ fibroblast cells compared to non-treated (None) *CathA*^{S190A} fibroblast cells. In these autophagy-related gene levels of both cell groups, after treatment with autophagy-inducing conditions, alterations were detected compared to their non-treated states (Figure 3.3).

3.2.2. Western Blot

Western Blot analyses for autophagy marker LC3 and p62 proteins were performed for *CathA*$^{+/+}$ and *CathA*^{S190A} mice-derived neuroglia and fibroblast cells.

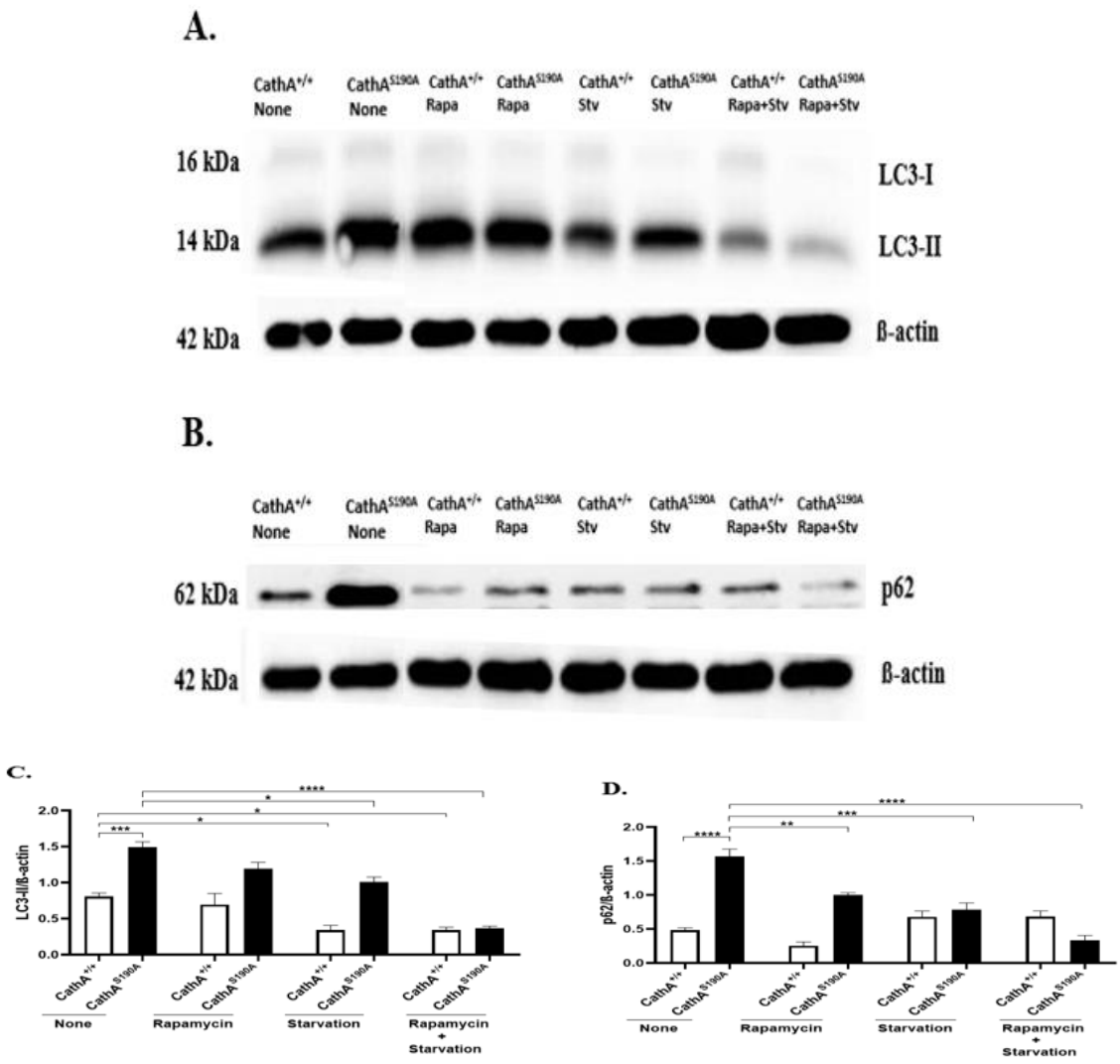

Figure 3.4. The representative Western Blot analysis for autophagy detection of *CathA*$^{+/+}$ and *CathA*^{S190A} neuroglia cells in non-treated (None) and autophagy-inducing Rapamycin (Rapa), Starvation (Stv) and Rapamycin+Starvation (Rapa+Stv) conditions. **(A)** Immunoblot analyses of LC3 and ß-actin proteins, **(B)** immunoblot analyses of p62 and ß-actin proteins, **(C)** densitometric analysis graph of LC3-II protein intensities which were normalized to ß-actin intensities and **(D)** densitometric analysis graph of p62 protein intensities which were normalized to ß-actin intensities. ß-actin was used as an internal loading control. (n=3;*p<0,05,**p<0,01,***p<0,001,****p<0,0001) Immunoblot gel images were processed using ImageJ, and the Two-way *ANOVA* analysis method was used to determine p-values via GraphPad Prism.

The anti-LC3 antibody (1:10000, Cell Signaling Technology, 2775S) which was used in our Western Blot analysis, indicated LC3-I, the cytosolic form of LC3, and LC3-II, the autophagosome-linked form of LC3 (Feng et al., 2014; Mizushima et al., 2011; Tanida et al., 2004).

LC3-II protein level of non-treated (None) *CathA*^{S190A} neuroglia cells was determined as significantly increased compared to non-treated (None) *CathA*$^{+/+}$ neuroglia cells. In *CathA*$^{+/+}$ neuroglia cells, under autophagy-inducing Starvation and Rapamycin+Starvation, the LC3-II protein level was statistically significantly decreased compared to the non-treated (none) condition, while no change in LC3-II protein level was observed after Rapamycin treatment. LC3-II, which was found to accumulate significantly in non-treated (None) *CathA*^{S190A} neuroglia cells compared to non-treated (None) *CathA*$^{+/+}$ neuroglia cells, was significantly decreased under all autophagy-inducing treatment conditions, however, there was no significant change in increased LC3-II protein level after Rapamycin treatment (Figure 3.4.A and C).

When *CathA*^{S190A} and *CathA*$^{+/+}$ neuroglia cells were compared in terms of p62 protein levels, the p62 protein level of non-treated (None) *CathA*^{S190A} neuroglia cells was found to be significantly higher than non-treated (None) *CathA*$^{+/+}$ neuroglia cells. While none of the autophagy-inducing Rapamycin, Starvation, and Rapamycin+Starvation treatment conditions led to significant change in the protein level of p62 in *CathA*$^{+/+}$ neuroglia cells compared to non-treated (None) condition, there was a slightly decreased p62 protein level in Rapamycin treatment and slightly increased p62 protein level in Starvation and Rapamycin+Starvation condition compared to non-treated (None) condition. In catalytically inactive *CathA*^{S190A} neuroglia cells, increased p62 protein level was statistically significantly reduced after autophagy-inducing Rapamycin, Starvation, and Rapamycin+Starvation treatment conditions compared to non-treated (None) condition (Figure 3.4.B and D).

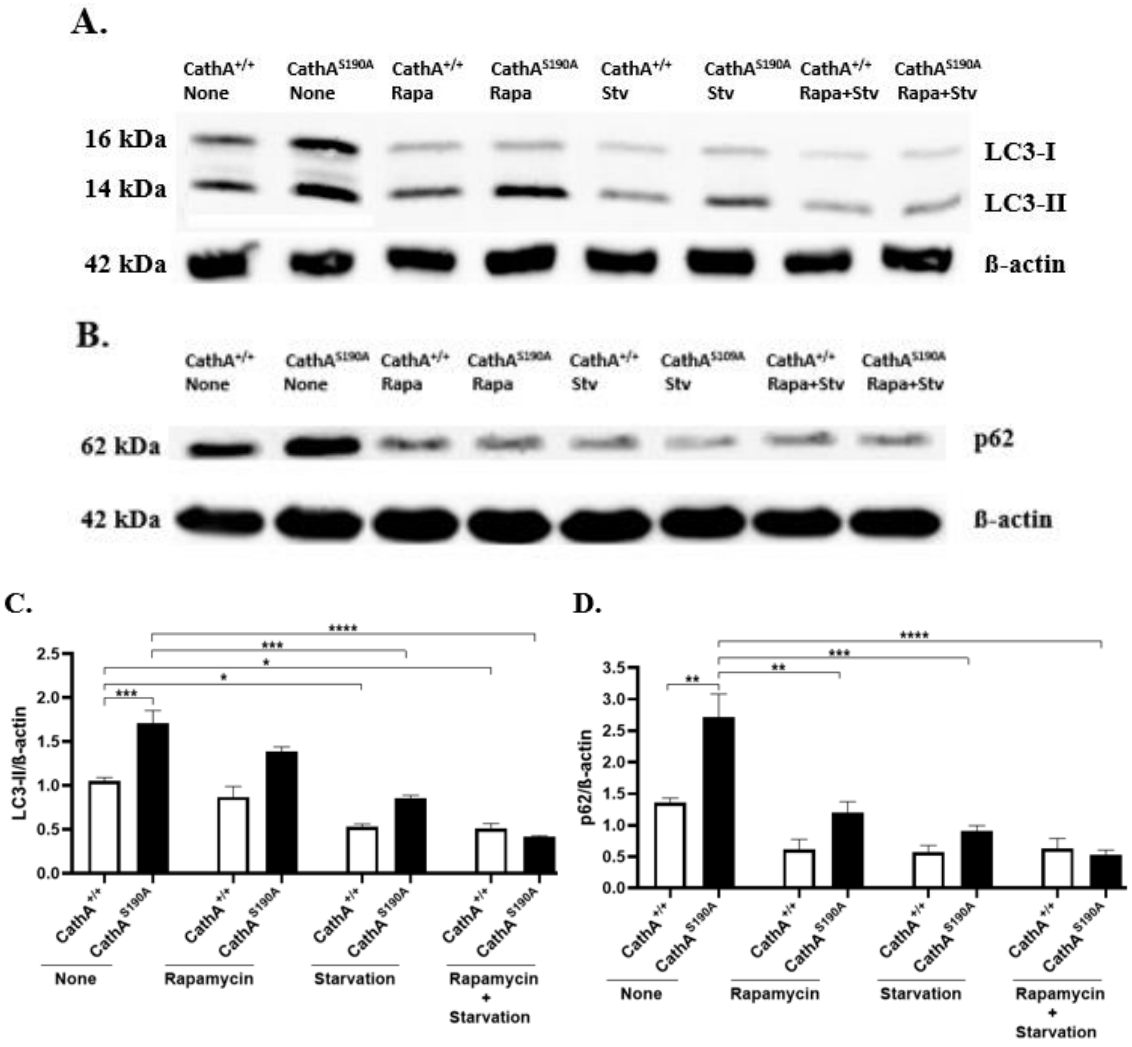

Figure 3.5. The representative Western Blot analysis for autophagy detection of *CathA*$^{+/+}$ and *CathA*^{S190A} fibroblast cells in non-treated (None) and autophagy-inducing Rapamycin (Rapa), Starvation (Stv) and Rapamycin+Starvation (Rapa+Stv) conditions. **(A)** Immunoblot analyses of LC3 and ß-actin proteins, **(B)** immunoblot analyses of p62 and ß-actin proteins, **(C)** densitometric analysis graph of LC3-II protein intensities which were normalized to ß-actin intensities and **(D)** densitometric analysis graph of p62 protein intensities which were normalized to ß-actin intensities. ß-actin was used as an internal loading control. (n=3;*p<0,05,**p<0,01,***p<0,001,****p<0,0001) Immunoblot gel images were processed using ImageJ, and the Two-way *ANOVA* analysis method was used to determine p-values via GraphPad Prism

As in neuroglia cell lines, the LC3-II protein level of non-treated (None) *CathA*^{S190A} fibroblast cells was significantly higher compared to non-treated (None) *CathA*$^{+/+}$ fibroblast cells. When control cells were treated under autophagy-inducing conditions, the LC3-II protein level was significantly reduced under Starvation and Rapamycin+Starvation conditions compared to the non-treated (None) condition, while a statistically insignificant decrease was observed after Rapamycin treatment. On the other hand, LC3-II protein level in *CathA*^{S190A} fibroblast cells was also significantly decreased under Starvation and Rapamycin+Starvation conditions, compared to the non-treated (None) condition, while there was no statistically significant change in the Rapamycin treatment condition (Figure 3.5.A and C).

The p62 protein level of non-treated (None) *CathA*^{S190A} fibroblast cells was significantly increased compared to non-treated (None) *CathA*$^{+/+}$ fibroblast cells. The autophagy-inducing conditions Rapamycin, Starvation, and Rapamycin+Starvation treatments resulted in a statistically insignificant reduction in p62 protein levels of control cells compared to the non-treated (None) condition. The accumulated p62 protein level in *CathA*^{S190A} fibroblast cells was statistically significantly decreased in all autophagy-inducing conditions compared to non-treated (None) condition of *CathA*^{S190A} fibroblast cells (Figure 3.5. B and D).

3.2.3. Immunocytochemistry (ICC)

Immunocytochemical analyses were performed to determine whether the autophagy mechanism is affected in the absence of the catalytic activity of the lysosomal Cathepsin A enzyme and, if so, to determine the accumulation of secondary autophagic substrates. Immunostaining and co-localized analysis of autophagy-related LC3-LAMP1 and p62-LAMP1 proteins were done in *CathA*$^{+/+}$ and *CathA*^{S190A} mice-derived neuroglia and fibroblast cells.

A.

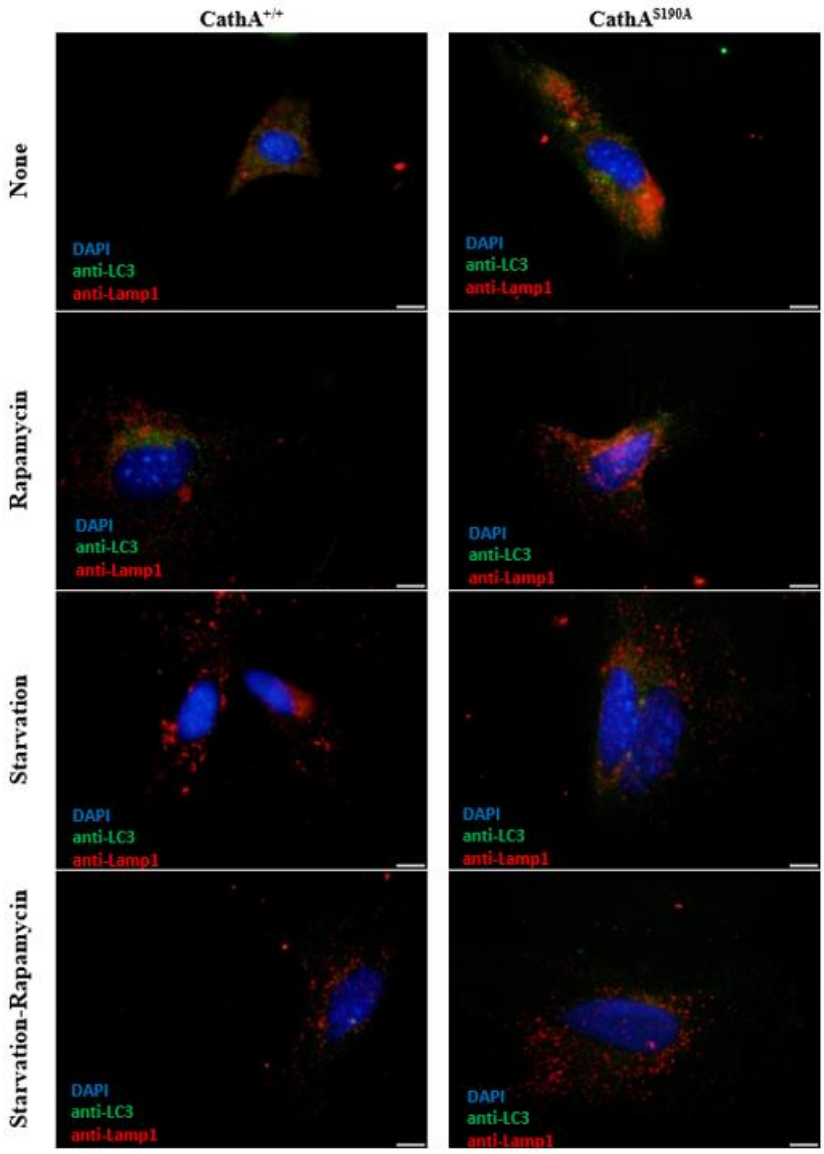
CathA+/+
CathAS190A
None
Rapamycin
Starvation
Starvation-Rapamycin
DAPI
anti-LC3
anti-Lamp1

B.

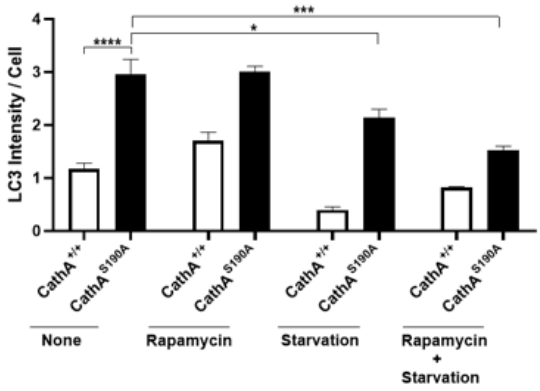
LC3 Intensity / Cell
0
1
2
3
4
****
*
***
CathA +/+
CathA S190A
None
Rapamycin
Starvation
Rapamycin + Starvation

C.

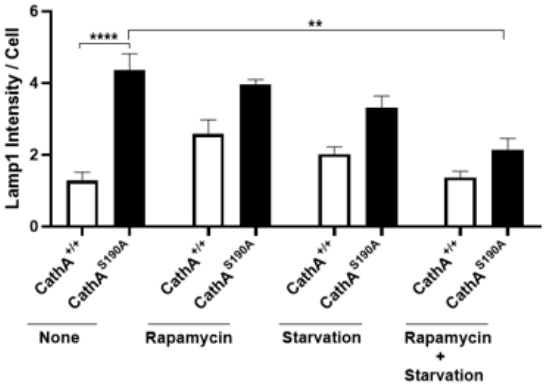
Lamp1 Intensity / Cell
0
2
4
6
****
**
CathA +/+
CathA S190A
None
Rapamycin
Starvation
Rapamycin + Starvation

Figure 3.6. (A) Immunostaining of LC3 and LAMP1 proteins in CathA$^{+/+}$ and CathA^{S190A} neuroglia cells. (B) LC3 (green fluorescent signals) protein intensity/cell graph. (C) LAMP1 (red fluorescent signals) protein intensity/cell graph. Images were taken at 100X magnification by using the same light intensity differing only in fluorescent filter type. Fluorescent signals of proteins were measured by using ImageJ and the Two-way *ANOVA* analysis method was used to determine p-values (*p<0,05,**p<0,01,***p<0,001,****p<0,0001).

It was determined that LC3 and LAMP1 protein intensity levels were significantly higher in non-treated (None) neuroglia cells isolated from catalytically deficient *CathA*^{S190A} mice compared to non-treated (None) *CathA*$^{+/+}$ neuroglia cells isolated from age-matched *CathA*$^{+/+}$ mouse (Figure 3.6.A, B and C).

While autophagy-inducing Rapamycin, Starvation, and Rapamycin+Starvation conditions did not cause a statistically significant decrease, compared to non-treated (none) condition, in LC3 protein intensity level of *CathA*$^{+/+}$ neuroglia cells which was reflected by protein-specific fluorescent signals, there was a slight increase after Rapamycin treatment and a slight decrease after Starvation and Rapamycin+Starvation conditions. In *CathA*^{S190A} neuroglia cells, compared to the non-treated (None) condition, the LC3 protein intensity level was found to be significantly reduced after Starvation and Rapamycin+Starvation treatment conditions, but no change was observed in the LC3 protein intensity level of *CathA*^{S190A} neuroglia cells after the Rapamycin treatment condition (Figure 3.6.A and B).

The intensity level of LAMP1 protein, which was used as a lysosome marker, in *CathA*$^{+/+}$ neuroglia cells increased in all autophagy-inducing treatment conditions compared to non-treated (None) condition, but these increases were not statistically significant. On the other hand, the LAMP1 protein intensity level in *CathA*^{S190A} neuroglia cells was also decreased in all autophagy-inducing treatment conditions compared to the non-treated (None) condition, while the decrease in LAMP1 protein intensity level after only the Rapamycin+Starvation condition was statistically significant (Figure 3.6.A and C).

A.

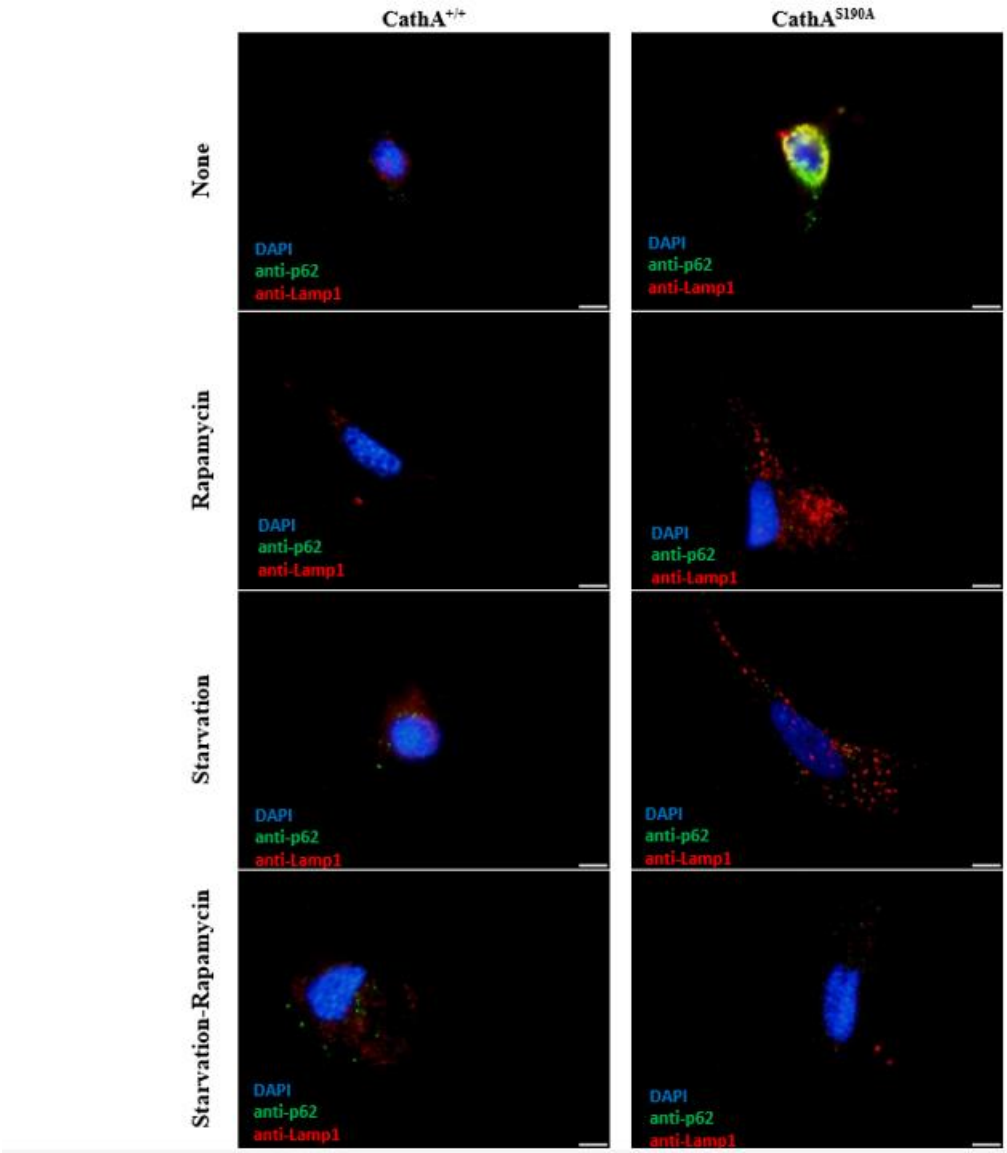
CathA+/+
CathA S190A
None
Rapamycin
Starvation
Starvation-Rapamycin
DAPI
anti-p62
anti-Lamp1

B.

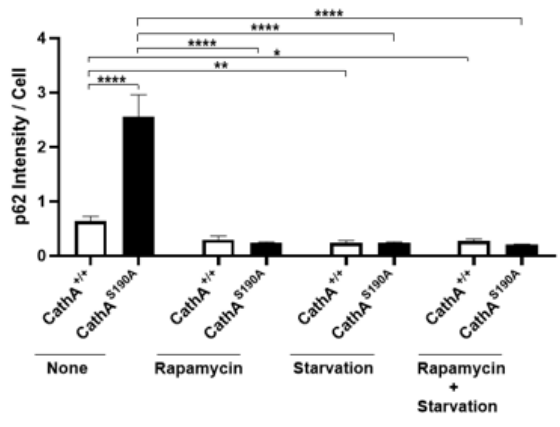
p62 Intensity / Cell
CathA +/+
CathA S190A
None
Rapamycin
Starvation
Rapamycin + Starvation

C.

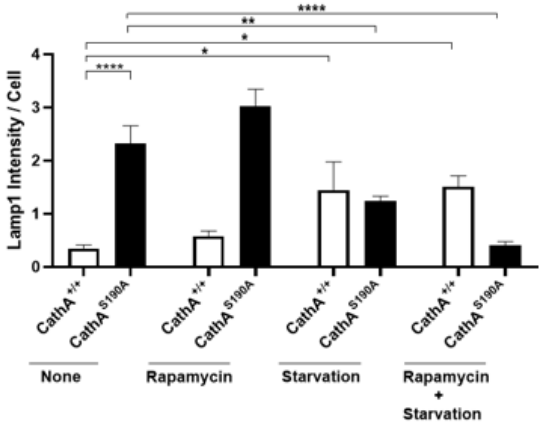
Lamp1 Intensity / Cell
CathA +/+
CathA S190A
None
Rapamycin
Starvation
Rapamycin + Starvation

Figure 3.7. (A) Immunostaining of p62 and LAMP1 proteins in *CathA*$^{+/+}$ and *CathA*^{S190A} neuroglia cells. (B) p62 (green fluorescent signals) protein intensity/cell graph. (C) LAMP1 (red fluorescent signals) protein intensity/cell graph. Images were taken at 100X magnification by using the same light intensity differing only in fluorescent filter type. Fluorescent signals of proteins were measured by using ImageJ and the Two-way *ANOVA* analysis method was used to determine p-values (*p<0,05,**p<0,01,***p<0,001,****p<0,0001).

The p62 protein intensity level of non-treated (None) *CathA*^{S190A} neuroglia cells was significantly high compared to non-treated (None) *CathA*$^{+/+}$ neuroglia cells. Autophagy-inducing Starvation and Rapamycin+Starvation treatment conditions resulted in a significant decrease in the p62 protein intensity level of *CathA*$^{+/+}$ neuroglia cells compared to non-treated condition. On the other hand, the protein intensity level of p62 significantly reduced in all of the autophagy-inducing conditions which were Rapamycin, Starvation, and Rapamycin+Starvation treatments, in *CathA*^{S190A} neuroglia cells compared to non-treated (None) condition (Figure 3.7. A and B).

In non-treated (None) *CathA*^{S190A} neuroglia cells the LAMP1 protein intensity level was also significantly increased compared to non-treated (None) *CathA*$^{+/+}$ neuroglia cells. It was determined that the LAMP1 protein intensity levels of *CathA*$^{+/+}$ neuroglia cells significantly increased after Starvation and Rapamycin+Starvation autophagy-inducing treatment conditions compared to non-treated (None) condition. As a contrast, the LAMP1 protein intensity level of *CathA*^{S190A} neuroglia cells was significantly decreased with Starvation and Rapamycin+Starvation treatment conditions compared to its non-treated (None) condition (Figure 3.7. A and C).

A.

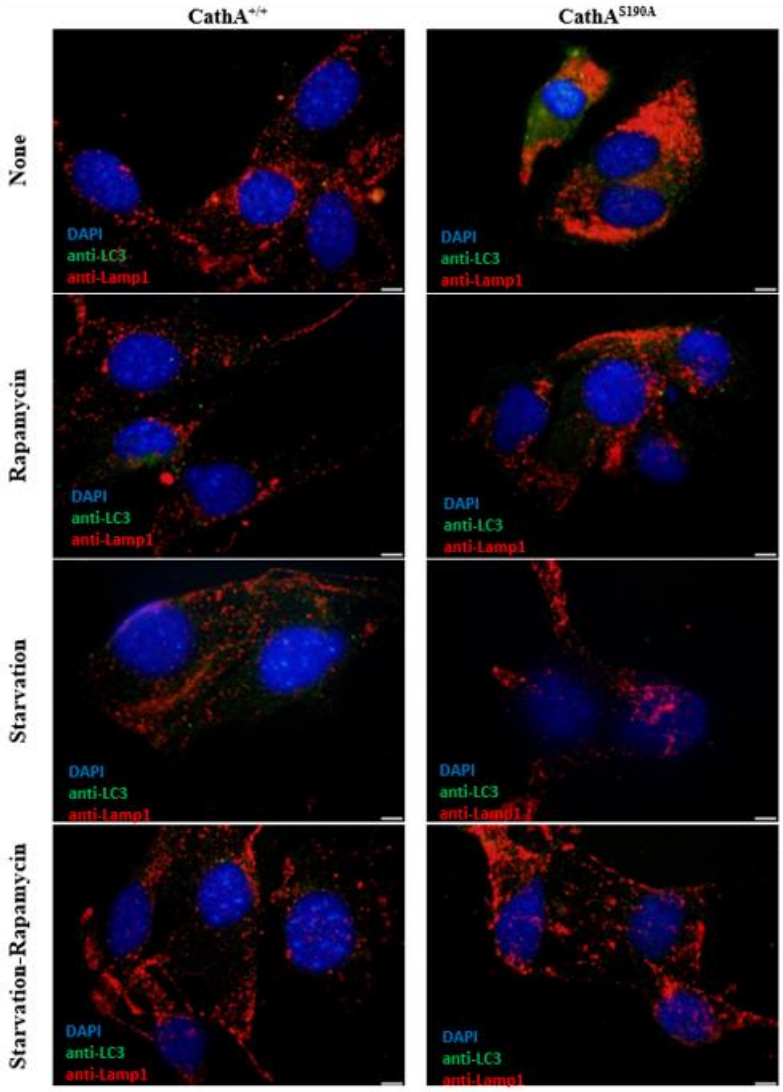
CathA+/+
CathAS190A
None
Rapamycin
Starvation
Starvation-Rapamycin
DAPI
anti-LC3
anti-Lamp1

B.

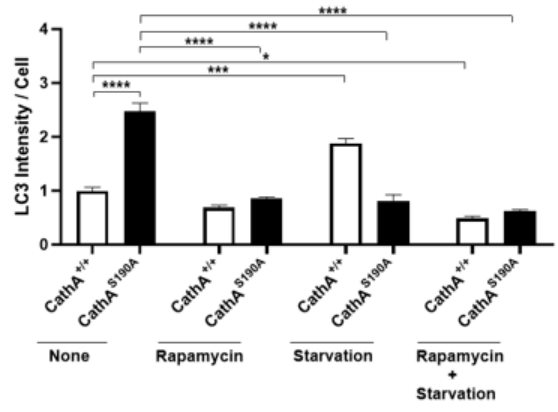
LC3 Intensity / Cell
CathA +/+
CathA S190A
None
Rapamycin
Starvation
Rapamycin + Starvation

C.

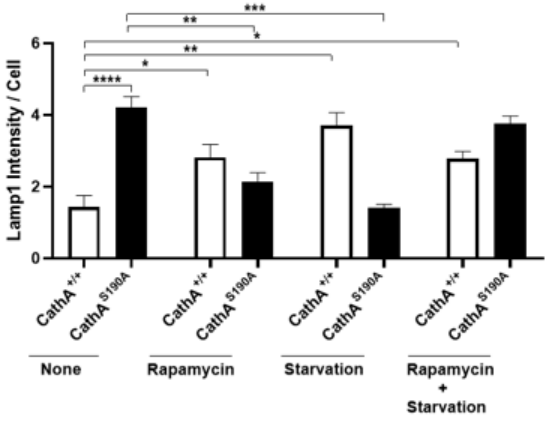
Lamp1 Intensity / Cell
CathA +/+
CathA S190A
None
Rapamycin
Starvation
Rapamycin + Starvation

Figure 3.8. (A) Immunostaining of LC3 and LAMP1 proteins in *CathA*$^{+/+}$ and *CathA*^{S190A} fibroblast cells. (B) LC3 (green fluorescent signals) protein intensity/cell graph. (C) LAMP1 (red fluorescent signals) protein intensity/cell graph. Images were taken at 100X magnification by using the same light intensity differing only in fluorescent filter type. Fluorescent signals of proteins were measured by using ImageJ and the Two-way *ANOVA* analysis method was used to determine p-values (*p<0,05,**p<0,01,***p<0,001,****p<0,0001).

The LC3 protein intensity level of non-treated (None) *CathA*^{S190A} fibroblast cells was significantly increased compared to non-treated (None) *CathA*$^{+/+}$ fibroblast cells. The level of LC3 protein intensity in *CathA*$^{+/+}$ fibroblast cells was significantly increased in the Starvation treatment condition compared to the non-treated (None) condition and statistically significantly decreased in the Rapamycin+Starvation treatment condition. There was no difference in LC3 protein intensity level in *CathA*$^{+/+}$ fibroblast cells treated with the rapamycin condition. On the other hand, the LC3 protein intensity level of CathA^{S190A} fibroblast cells decreased significantly compared to non-treated (None) condition after all autophagy-inducing treatment conditions (Figure 3.8.A and B).

As a result of the immunocytochemical staining and analyses we performed, it was observed that the intensity level of LAMP1 protein, which is a lysosome marker protein, increased significantly in non-treated (None) *CathA*^{S190A} fibroblast cells compared to non-treated (None) *CathA*$^{+/+}$ fibroblast cells. After all autophagy-inducing treatment conditions, it was determined that the LAMP1 protein intensity level in *CathA*$^{+/+}$ fibroblast cells was significantly increased compared to the non-treated (none) condition. The LAMP1 protein intensity levels of CathA^{S190A} fibroblast cells were significantly reduced after the Rapamycin and Rapamycin+Starvation treatment conditions compared to the non-treated (none) condition, but did not change significantly after the Starvation treatment condition (Figure 3.8.A and C).

A.

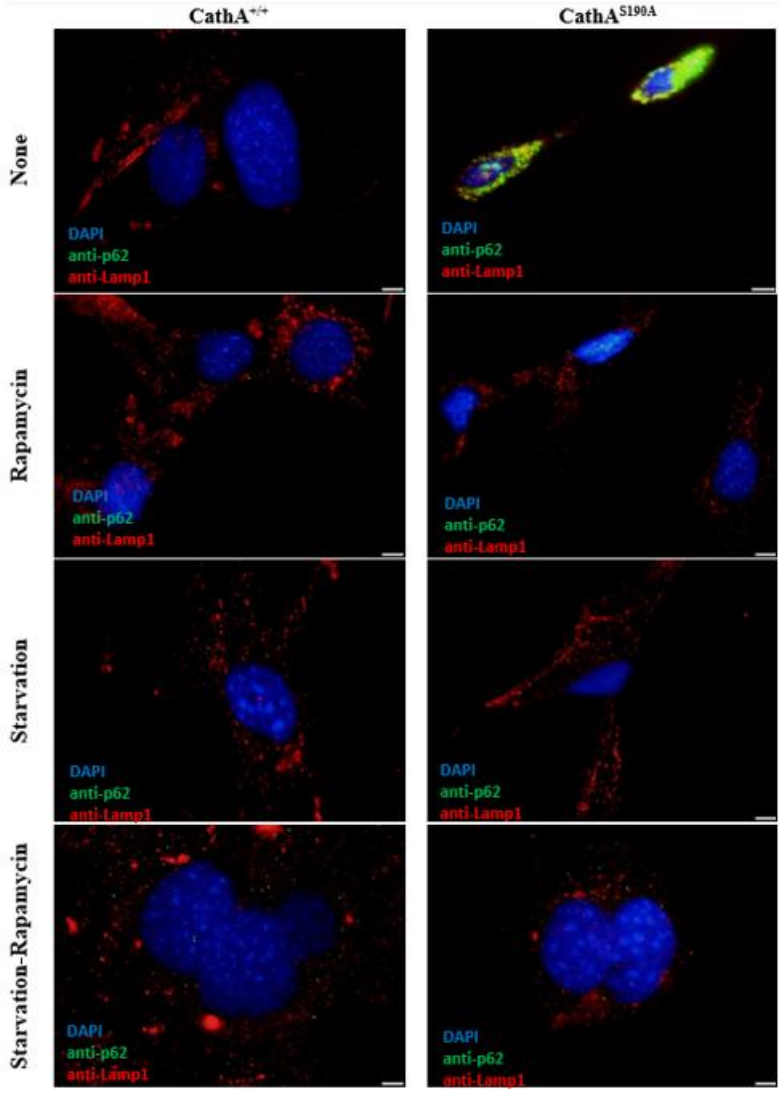
CathA+/+
CathA S190A
None
Rapamycin
Starvation
Starvation-Rapamycin
DAPI
anti-p62
anti-Lamp1

B.

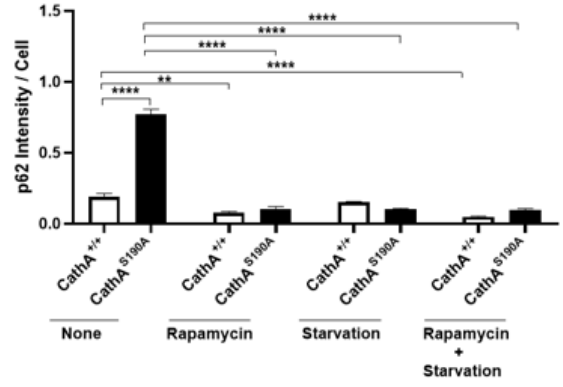
p62 Intensity / Cell
1.5
1.0
0.5
0.0
****
****
****
****
**
****
CathA +/+
CathA S190A
None
Rapamycin
Starvation
Rapamycin + Starvation

C.

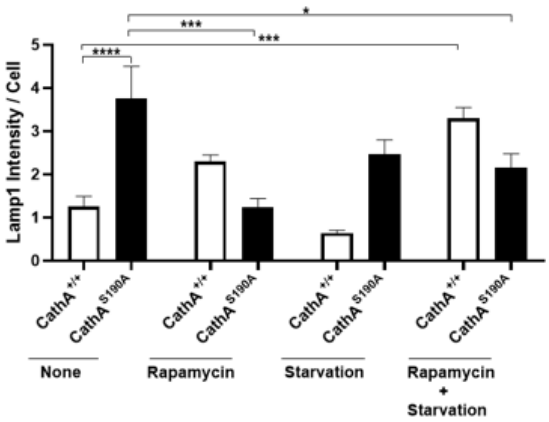
Lamp1 Intensity / Cell
5
4
3
2
1
0
*
***
***
****
CathA +/+
CathA S190A
None
Rapamycin
Starvation
Rapamycin + Starvation

Figure 3.9. (A) Immunostaining of p62 and LAMP1 proteins in *CathA*$^{+/+}$ and *CathA*^{S190A} fibroblast cells. (B) p62 (green fluorescent signals) protein intensity/cell graph. (C) LAMP1 (red fluorescent signals) protein intensity/cell graph. Images were taken at 100X magnification by using the same light intensity differing only in fluorescent filter type. Fluorescent signals of proteins were measured by using ImageJ and the Two-way *ANOVA* analysis method was used to determine p-values (*p<0,05,**p<0,01,***p<0,001,****p<0,0001).

The p62 protein intensity level of non-treated (None) *CathA*^{S190A} fibroblast cells was significantly high compared to non-treated (None) *CathA*$^{+/+}$ fibroblast cells. The level of p62 protein intensity in *CathA*$^{+/+}$ fibroblast cells after Rapamycin and Rapamycin+Starvation treatment conditions was significantly reduced compared to the non-treated (None) condition, while there was no statistically significant change after the Starvation treatment condition. After the autophagy-inducing Rapamycin, Starvation, and Rapamycin+Starvation conditions, the p62 protein intensity level of *CathA*^{S190A} fibroblast cells was statistically reduced compared to the non-treated (none) condition (Figure 3.9.A and B).

Non-treated (none) *CathA*^{S190A} fibroblast cells' LAMP1 protein intensity level was significantly increased rather than the LAMP1 protein intensity level of non-treated (none) *CathA*$^{+/+}$ fibroblast cells. After autophagy-inducing conditions were applied to *CathA*$^{+/+}$ fibroblast cells, only the Rapamycin+Starvation treatment condition showed a significant change, increasing the LAMP1 protein intensity level compared to the non-treated (none) condition; there was an insignificant increase in the LAMP1 protein intensity level of the *CathA*$^{+/+}$ fibroblast cells after the Rapamycin treatment condition, while there was an insignificant increase in the LAMP1 protein intensity level of the *CathA*$^{+/+}$ fibroblast cells after the Starvation treatment condition compared to non-treated (none) condition. The LAMP1 protein intensity level of *CathA*^{S190A} fibroblast cells was significantly decreased after autophagy-inducing Rapamycin and Rapamycin+Starvation treatment conditions, there was an insignificant decrease with Starvation treatment condition compared to non-treated (none) condition (Figure 3.9.A and C).

CHAPTER 4

DISCUSSION

Serine protease family member lysosomal Cathepsin A which is known as shortly CathA or PPCA, is a multifunctional enzyme with distinct protective and catalytic functions (Hiraiwa et al., 1999). It forms a lysosomal multienzyme complex (LMC) with Neuraminidase-1 (Neu1) and ß-Galactosidase (ß-Gal) enzymes to protect them from hydrolytic degradation in the highly acidic lysosome. Also, it has a pivotal role in the routing of the Neu1 enzyme to the lysosome and enzymatic activation and stabilization of the Neu1 enzyme (D'Azzo et al., 1982; Bonten et al., 2014). Lysosomal CathA enzyme has carboxypeptidase activity at acidic pH values (4.5-5.5) and deamidase/esterase activity at neutral pH values on the degradation of a group of short bioactive peptides such as Endothelin-1, substance P and oxytocin (Jackman et al., 1990). Lysosomal Cathepsin A plays a role in the hydrolytic inhibition of vasoactive peptides which are endothelin-1, bradykinin, and angiotensin, and neuropeptides which are oxytocin and substance P (Bonten et al., 2014).

$CathA^{S190A}$ is a catalytically inactive knock-in Cathepsin A mouse model in which serine on the aminoacid position of 190 was replaced with alanine as a point mutation. $CathA^{S190A}$ mouse model is only mutated in its catalytic function; the protective function is preserved to form LMC with Neu1 and ß-Gal enzymes (Seyrantepe et al., 2008). *In vivo* role of lysosomal CathA enzyme on the degradation of short bioactive peptides was firstly studied in the $CathA^{S190A}$ mouse model: vasoactive and neuropeptides significantly accumulate in the different tissues and serum of the 3- and 6-month-old $CathA^{S190A}$ and their WT littermates. Also, hippocampal accumulation of endothelin-1 and oxytocin peptides were shown in 3-, 6- and 12-month-old $CathA^{S190A}$ mice compared with age-matched WT mice, and accumulation of these peptides was associated with several cognitive inabilities in $CathA^{S190A}$ mice.

Autophagy is an intracellular and lysosome-routed process for degradation and recycling into the building blocks of lipids, proteins, nucleic acids, damaged or superfluous organelles, etc. to maintain cellular homeostasis (Ichimiya et al., 2020). Autophagy is mainly divided into the 3 subtypes which are macroautophagy, microautophagy, and chaperone-mediated autophagy (CMA) and unless otherwise stated,

autophagy refers to macroautophagy. Unlike microautophagy and CMA, in the macroautophagy pathway, the substrates to be degraded are transported to the lysosome by double-membrane structures called "autophagosome" and fuse the autophagosome with the lysosome, resulting in the enzymatic hydrolyze of the cellular cargoes (Parzych and Klionsky, 2014). Autophagic machinery is evolutionary conserved and tightly regulated in eukaryotic cells (King, 2012). Autophagic machinery is initiated with phagophore formation, elongated with complete closure of the autophagosome membrane, and terminated with the fusion of autophagosome and lysosome to degrade intracellular components (Yu et al., 2018; Sengul et al., 2023). Cuervo and her colleagues have shown that Cathepsin A has a regulatory role on the CMA via hydrolyzing of the Lamp2a which is a rate-limiting factor of CMA (Cuervo et al., 2003). In order to understand whether the lysosomal Cathepsin A enzyme has a role in the regulation of the autophagy mechanism *in vitro*, the autophagic flux in neuroglia and fibroblast cell lines we established from the $CathA^{S190A}$ mouse, which is a mouse model with the catalytically inactive Cathepsin A enzyme, were compared with $CathA^{+/+}$ mouse' neuroglia and fibroblast cell lines analyzing Western Blot, RT-PCR and Immunocytochemistry (ICC) methods for the first time.

Beclin-1 is a member of the lipid kinase complex which is Beclin-1-Vps34-Vps35 and Beclin-1 has a role in the initiation of autophagy by inducing vesicle nucleation (Del Grosso et al., 2019; Lee et al., 2015). Our gene expression analyses using the quantitative RT-PCR method have shown that the gene expression level of Beclin-1 in $CathA^{S190A}$ neuroglia cells was significantly increased compared to $CathA^{+/+}$ neuroglia cells (Figure 3.2.A), while the Beclin-1 gene expression level in $CathA^{S190A}$ fibroblast cells was significantly lower compared to $CathA^{+/+}$ fibroblast cells (Figure 3.3.A). In Pompe disease, a lysosomal storage disease, analysis of muscle biopsy samples of patients has shown that the Beclin-1 gene expression level is upregulated (Nascimbeni et al., 2012). In the Hexa-/-Neu3-/- mouse, which is an early onset mouse model of Tay-Sachs disease, the level of Beclin-1 gene expression was analyzed in 4 different brain regions (cortex, cerebellum, thalamus, and hippocampus) of 2 and 5-month-old mice compared to age-matched WT mice and it was shown that transcription level of Beclin-1 was both up and downregulated in different brain region and different age of mice (Sengul et al., 2023). The deficiency of catalytic activity of the lysosomal Cathepsin A enzyme causes alterations in the transcriptional expression of the Beclin-1 gene by showing different patterns in neuroglia and fibroblast cells which were established from the catalytically

inactive CathA^{S190A} mouse, compared to the CathA$^{+/+}$ neuroglia and fibroblast cells. When autophagy-inducing Rapamycin, Starvation, and Rapamycin+Starvation conditions were applied to CathA^{S190A} neuroglia cells, the increased Beclin-1 gene expression level was significantly decreased in all autophagy-inducing conditions compared to non-treated (None) CathA^{S190A} neuroglia cells (Figure 3.2.A). Especially after the Starvation treatment condition, Beclin-1 gene expression levels in CathA^{S190A} and CathA$^{+/+}$ neuroglia cells were found to be very close to each other ((Figure 3.2.A). None of the autophagy-inducing conditions significantly altered the Beclin-1 gene expression level of Cathepsin cells compared to the non-treated (None) condition, but the Starvation treatment condition slightly increased the Beclin-1 gene expression level, while the expression level of the Beclin-1 gene was slightly decreased after the Rapamycin+Starvation condition (Figure 3.3.A). As a result, while the expression level of Beclin-1 in CathA^{S190A} neuroglia cells responded significantly to all autophagy-inducing conditions, no statistically significant change was observed in CathA^{S190A} fibroblast cells under autophagy-inducing conditions. The closest Beclin-1 gene expression pattern in both of CathA^{S190A} neuroglia and fibroblast cells was observed under Starvation condition.

Atg9 is a transmembrane protein and has a pivotal role in the initiation of autophagy by recruiting the lipids forming the bilayer structure of the autophagosome from donor sources and Atg9 serves as a membrane scaffold for the autophagosome formation (Feng et al., 2014; Mari et al., 2011; Orsi et al., 2010). Quantitative RT-PCR analyses we performed revealed that the Atg9 gene expression level in CathA^{S190A} neuroglia cells was significantly high compared to CathA$^{+/+}$ neuroglia cells and the gene expression level of Atg9 was low in CathA^{S190A} fibroblast cells compared to CathA$^{+/+}$ fibroblast cells (Figure 3.2.B and 3.3.B). In studies of Hexa-/-Neu3-/- mice, an early-onset mouse model of Tay-Sachs disease and shown to have impaired autophagic flux, the level of Atg9 gene expression in the cerebellum of 2-month-old Hexa-/-Neu3-/- mice was significantly high compared to 2-month-old WT mice. On the other hand, the Atg9 gene expression level in the cerebellum of 5-month-old Hexa-/-Neu3-/- mice was significantly reduced compared to 5-month-old WT mice (Sengul et al., 2023). Like the changes in the Beclin-1 gene expression level, it has been observed that the deficiency of the catalytic activity of the Cathepsin A enzyme causes alterations in CathA^{S190A} neuroglia and fibroblast cells, albeit with different patterns. Autophagy-inducing Rapamycin, Starvation, and Rapamycin+Starvation treatment conditions have resulted in

a significant decrease in the gene expression level of Atg9 in CathA^{S190A} neuroglia cells compared to non-treated (none) condition and the most similar Atg9 gene expression level in CathA$^{+/+}$ neuroglia cells were seen in CathA^{S190A} neuroglia cells treated with the Starvation condition (Figure 3.2.B). In CathA^{S190A} fibroblast cells, the gene expression level of Atg9 was slightly but not significantly decreased with Rapamycin and Starvation treatment conditions, as a contrast, the Atg9 gene expression level of CathA^{S190A} fibroblast cells significantly increased in the Rapamycin+Starvation treatment condition (Figure 3.3.B). In conclusion, the Atg9 gene expression profile was altered in both of catalytically inactive CathA^{S190A} mouse-derived neuroglia and fibroblast cells compared to CathA$^{+/+}$ neuroglia and fibroblast cells but with different expression patterns.

Atg7 is an E1-like enzyme and is involved in the cytosolic LC3-I conversion to the autophagosome-associated LC3-II with the addition of phosphatidylethanolamine (PE) (Feng et al., 2014). Our RT-PCR data have shown that the gene expression level of Atg7 was significantly high in CathA^{S190A} neuroglia cells compared to CathA$^{+/+}$ neuroglia cells (Figure 3.2.C). On the contrary, CathA^{S190A} fibroblast cells' Atg7 gene expression level was significantly decreased compared to CathA$^{+/+}$ fibroblast cells (Figure 3.3.C). In the cerebellum, cortex, hippocampus, and thalamus brain regions of 2- and 5-month-old Hexa-/-Neu3-/- mice, which is an early-onset mouse model Tay-Sachs disease, have shown altered Atg7 gene expression profile (Sengul et al., 2023). Deficiency of catalytic activity of lysosomal Cathepsin A enzyme resulted in the alterations in the gene expression profile of Atg7 in neuroglia and fibroblast cells of CathA^{S190A} mouse compared to CathA$^{+/+}$ mouse. The Atg7 gene expression level in CathA^{S190A} neuroglia cells increased significantly after Rapamycin and Rapamycin+Starvation conditions and slightly increased after the Starvation treatment condition compared to the non-treated (None) condition (Figure 3.2.C). In CathA^{S190A} fibroblast cells, the gene expression level of Atg7 significantly increased after the Rapamycin+Starvation treatment condition compared to the non-treated (None) condition (Figure 3.3.C). Our results suggest that especially autophagy-inducing Starvation and Rapamycin+Starvation conditions increased the Atg7 gene expression level in catalytically inactive CathA^{S190A} neuroglia and fibroblast cells.

p62, known as SQSTM1/p62, recruits the ubiquitinated cargo into the forming autophagosomes in the selective autophagy by interacting with LC3-II (Bjørkøy et al., 2006). Our transcriptional analyses related to the p62 gene expression ratio have shown that the gene expression level of p62 in CathA^{S190A} neuroglia cells was significantly high

compared to CathA$^{+/+}$ neuroglia cells (Figure 3.2.D). Surprisingly, in CathA^{S190A} fibroblast cells, the gene expression level of p62 is significantly lower than in CathA$^{+/+}$ neuroglia cells' (Figure 3.3.D). Pompe disease patients' muscle biopsy samples showed transcriptionally upregulated p62 levels (Nascimbeni et al., 2012). Also, the early-onset Tay-Sachs mouse model, Hexa-/-Neu3-/- mouse, showed higher p62 gene expression levels in cerebellum, hippocampus, and thalamus brain regions of 2- and 5-month-old mice compared to age-matched WT counterparts (Sengul et al., 2023). Our qRT-PCR analyses have revealed that the catalytic activity of the lysosomal Cathepsin A enzyme leads to alterations in the gene expression level of p62 in neuroglia and fibroblast cells. It was determined that the p62 gene expression level was significantly increased in both CathA^{S190A} neuroglia and fibroblast cells in Starvation and Rapamycin+Starvation treatment conditions, which are autophagy-inducing conditions, compared to non-treated (none) conditions of the cell lines. After the rapamycin treatment condition, the p62 gene expression level was significantly increased in CathA^{S190A} neuroglia cells, while no difference was observed in CathA^{S190A} fibroblast cells (Figure 3.2.D and 3.3.D). In conclusion; Starvation, and Rapamycin+Starvation treatment conditions have induced autophagic biogenesis via autophagy marker p62 gene expression.

Lysosomal associated membrane protein-2 (LAMP2) gene encodes lysosomal transmembrane proteins and the mutations affecting the LAMP2 gene, lead to glycogen-stored lysosomal storage disease, Danon disease. It has a tissue-specific expression pattern and differs in tissue or cell types (Eskelinen, 2006). LAMP2 gene's transcriptional product is a rate-limiting factor of CMA and lysosomal CathA enzyme has catalytic activity on the degradation of LAMP2 protein (Cuervo et al., 2003). Deficiency of catalytic activity of CathA enzyme have resulted in different LAMP2 gene expression levels in neuroglia and fibroblast cells compared to their CathA$^{+/+}$ counterparts: the gene expression level of LAMP2 gene in CathA^{S190A} neuroglia cells significantly reduced compared to CathA$^{+/+}$ neuroglia cells, on the other hand, significantly reduced LAMP2 gene expression level was analyzed in CathA^{S190A} fibroblast cells compared to CathA$^{+/+}$ fibroblast cells (Figure 3.2.E and 3.3.E). Significantly increased LAMP2 gene expression was reported in Hexa-/-Neu3-/- mice which is an early-onset Tay-Sachs mouse model (Seyrantepe et al., 2018). Like other autophagy-related genes, we analyzed in this study, the LAMP2 gene expression level was altered in both CathA^{S190A} mice-derived neuroglia and fibroblast cells with different expression patterns. None of the autophagy-inducing conditions were found to cause a significant change in the LAMP2 gene expression level

of neither CathA^{S190A} neuroglia nor CathA^{S190A} fibroblast cells compared to non-treated (none) condition (Figure 3.2.E and 3.3.E). When the CathA^{S190A} neuroglia or fibroblast cells were treated with Rapamycin, Starvation, or Rapamycin+Starvation conditions, significant changes were observed in the expression levels of other autophagy-related genes, Beclin-1, Atg9, Atg7, and p62, while no significant change was observed in the LAMP2 gene expression level. We think that this is due to the fact that the LAMP2 protein is a known substrate of the lysosomal Cathepsin A enzyme. The other autophagy-related genes we analyzed in this thesis study do not have a known substrate relationship with the lysosomal Cathepsin A enzyme. Therefore, we conclude that the increased LAMP2 protein level in the absence of Cathepsin A enzyme, previously shown by Cuervo et al, does not significantly change the gene expression level of LAMP2 in conditions that trigger basal autophagy with the catalytically inactive Cathepsin A enzyme.

In conclusion regarding our quantitative RT-PCR results which we performed for catalytically inactive CathA^{S190A} neuroglia and fibroblast cells compared with CathA$^{+/+}$ counterparts: the deficiency of catalytic activity of lysosomal Cathepsin A enzyme results in alterations in the autophagic biogenesis in meaning of transcriptional level for the autophagy-related Beclin-1, Atg9, Atg7, p62 and LAMP2 genes. These changes showed different expression patterns in CathA^{S190A} neuroglia and fibroblast cells compared to CathA$^{+/+}$ cells. We think that the reason for the different expression patterns for the autophagy-related genes that we analyzed in neuroglia and fibroblast cells with catalytically deficient lysosomal Cathepsin A enzyme, compared to CathA$^{+/+}$ cells, is due to the different expression levels of autophagy-related genes at the basal level in CathA$^{+/+}$ neuroglia and fibroblast cells. Because the expression levels of autophagy-related genes in both CathA^{S190A} neuroglia and CathA^{S190A} fibroblast cells are very close to each other, the expression levels of these genes in CathA$^{+/+}$ neuroglia and CathA$^{+/+}$ fibroblast cells are very different from each other. This may be related to the fact that the basal level of autophagy is different in different cell types and therefore the expression levels of autophagy-related genes are also different. Another reason why the transcriptional levels of autophagy-related genes are different at basal level in CathA$^{+/+}$ neuroglia and fibroblast cells may be related to the different expression of lysosomal Cathepsin A at gene and protein levels in these cell types. As a conclusion, the deficiency of catalytic activity of lysosomal Cathepsin A enzyme has led to alterations in the transcriptional level of autophagy-related genes in neuroglia and fibroblast cells. Additionally, it has been determined that autophagy-inducing Starvation and Rapamycin+Starvation conditions

may restore the altered expression levels of autophagy-related genes in CathA^{S190A} neuroglia and fibroblast cells.

We analyzed the autophagic LC3 and p62 proteins using Western Blot and Immunocytochemistry methods and LAMP1 protein using the Immunocytochemistry method in order to investigate whether there is an impairment in the autophagic flux in the deficiency of catalytic activity of lysosomal Cathepsin A enzyme in neuroglia and fibroblast cells. LC3 protein is involved in the formation and elongation of autophagosomes and is also required for the fusion of autophagosomes and lysosomes (Feng et al., 2014). In the autophagic machinery, extra-autophagosome linked LC3-II is converted to cytosolic LC3-I, and intra-autophagosome linked LC3-II is hydrolyzed by lysosomal enzymes. The protein level of LC3-II is evaluated as an autophagosomal marker of autophagy and is frequently used for monitoring the autophagic flux (Yoshii and Mizushima, 2017). Ubiquitin-binding scaffold protein p62 transports the ubiquitinated autophagic substrates into the formed autophagosome by interacting with LC3-II and the p62 protein level is analyzed to monitor the autophagic flux also, especially for the termination of autophagy (Bjørkøy et al., 2006; Bitto et al., 2014). LAMP-1 is a lysosomal integral membrane protein that is a commonly used lysosome marker in autophagic studies (Eskelinen, 2006). Increased LAMP1 protein levels and disturbed turnover of LAMP1 have been shown in several impaired autophagic flux lysosomal storage diseases such as Niemann-Pick type C disease patients' fibroblasts (Pugach et al., 2018), Pompe disease patients' fibroblasts (Meikle et al., 1999), Cystinosis mouse model (Ctsn$^{-/-}$) fibroblast cells and tissue samples (Napolitano et al., 2015). Studies have proven that secondary accumulation of autophagic substrate proteins, such as LC3-II and p62, is a common case in the defected or impaired autophagic flux such as several lysosomal storage diseases (LSD) (Settembre et al., 2008; Fukuda et al., 2006).

Our Western Blot results have revealed that LC3-II protein, which is an autophagosome-associated form of LC3 protein (Yoshii and Mizushima, 2017), was accumulated in CathA^{S190A} neuroglia cells compared to CathA$^{+/+}$ neuroglia cells (Figure 3.4.A and C). Also, it was determined that the LC3-II protein level of CathA^{S190A} fibroblast cells was significantly increased compared to CathA$^{+/+}$ fibroblast cells (Figure 3.5.A and C). Immunocytochemical analysis results we performed in these neuroglia and fibroblast cells for the protein level of LC3 also confirmed the Western Blot results: There was a significantly high number of LC3(+) vesicles in both of the CathA^{S190A} neuroglia and CathA^{S190A} fibroblast cells compared to CathA$^{+/+}$ counterparts (Figure 3.6 A and B,

Figure 3.8.A and B). As mentioned before, the protein level of LC3 represents the accumulation of autophagosomes (Sengul et al., 2023) and the accumulation of autophagosomes previously reported in various LSDs which autophagic flux is impaired and resulting from mutations in lysosomal enzymes such as Pompe disease (Fuduka et al., 2006), type IIIA mucopolysaccharidoses (Settembre et al., 2008), Danon disease (Tanaka et al., 2000), type IV mucolipidosis (Jennings Jr et al., 2006) and mouse model of Tay-Sachs disease (Sengul et al., 2023). Our study demonstrated, consistent with previous studies, significantly accumulated protein level of LC3-II in the catalytically inactive Cathepsin A mouse model, $CathA^{S190A}$, derived neuroglia and fibroblast cells and proportionally with this accumulated LC3 protein, increased number of autophagosomes in these $CathA^{S190A}$ neuroglia and fibroblast cells compared to $CathA^{+/+}$ neuroglia and fibroblast cells. When the $CathA^{S190A}$ neuroglia and fibroblast cells were treated with autophagy-inducing conditions; according to the Western Blot results, while it was observed that accumulated LC3 protein in Starvation and Rapamycin+Starvation conditions decreased significantly, there was no significant decrease in these cell groups after Rapamycin condition compared to non-treated (none) condition (Figure 3.4.A and C, Figure 3.5.A and C). On the other hand, our Immunocytochemical analyses have shown that while the Starvation and Rapamycin+Starvation treatment conditions significantly reduced the accumulated LC3 protein in $CathA^{S190A}$ neuroglia cells, all of the autophagy-inducing conditions which were Rapamycin, Starvation, and Rapamycin+Starvation, significantly reduced the protein level of the LC3 in $CathA^{S190A}$ fibroblast cells compared to non-treated (None) condition. Considering all these results, it may be said that autophagy-inducing Starvation and Rapamycin+Starvation conditions are more effective in the clearance of the significantly accumulated LC3 protein in both $CathA^{S190A}$ neuroglia and fibroblast cells.

The protein level of p62 was significantly increased in both the $CathA^{S190A}$ neuroglia and fibroblast cells compared to their $CathA^{+/+}$ counterparts (Figure 3.4.B and D, Figure 3.5.B and D). Also, the Immunocytochemical analyses we performed have shown the accumulated level of p62 protein in $CathA^{S190A}$ neuroglia and fibroblast cells compared to $CathA^{+/+}$ neuroglia and fibroblast cells, respectively (Figure 3.7 A and B, Figure 3.9.A and B). p62/SQSTM1 protein transports the ubiquitinated autophagic cargo into the autophagosome and is generally associated with the termination of autophagy (Sengul et al., 2023; Feng et al., 2014). Like other autophagic proteins, degradation of the p62 protein takes place in the termination of autophagic machinery along with

ubiquitinated autophagic substrates (Bjørkøy et al., 2006). Significantly increased level of the p62 protein has been previously reported in the various LSDs resulting from deficiency of the lysosomal enzymes, such as in Gaucher disease mouse model brain (Sun and Grabowski, 2010), $Npc^{-/-}$ mouse brain (Liao et al., 2007), Pompe disease mouse model muscle fibers (Raben et al., 2008), Fabry disease patients fibroblasts (Chévrier et al., 2010), type IV mucolipidosis disease patients fibroblast (Vergarajauregui et al., 2008) and Tay-Sachs disease mouse model brain (Sengul et al., 2023). Elevated levels of p62/SQSTM1 protein in $CathA^{S190A}$ neuroglia and fibroblast cells which is consistent with previous studies, have demonstrated the impairment in the termination of autophagic flux in the deficiency of catalytic activity of lysosomal Cathepsin A enzyme. According to the Western Blot analyses we performed; Rapamycin, Starvation, and Rapamycin+Starvation conditions, which are autophagy-inducing conditions, statistically significantly decreased the increased p62 protein level in $CathA^{S190A}$ neuroglia cells. As a parallel to the Western Blot results, according to the Immunocytochemistry analyses we performed, it was observed that the p62 protein level decreased significantly under all autophagy-inducing conditions compared to non-treated (none) condition (Figure 3.4.B and D, Figure 3.7.A and B). In the $CathA^{S190A}$ fibroblast cells, both the Western Blot and Immunocytochemical analyses have demonstrated that Rapamycin, Starvation, and Rapamycin+Starvation treatment conditions led to a significant decrease in the elevated p62 protein level compared to non-treated (none) condition (Figure 3.5.B and D, Figure 3.9.A and B). These analyses show that in $CathA^{S190A}$ neuroglia cells, especially Starvation and Rapamycin+Starvation conditions are effective treatment conditions for the clearance of the accumulated p62 proteins, while in $CathA^{S190A}$ fibroblast cells, all autophagy-inducing conditions are effective to restore the accumulated p62 protein level. LAMP1 protein level, which is one of the proteins we analyzed during immunocytochemical analyzes, was found to be significantly higher in both $CathA^{S190A}$ neuroglia cells and $CathA^{S190A}$ fibroblast cells compared to $CathA^{+/+}$ cells (Figure 3.6.A and C, Figure 3.8.A and C). Increased LAMP1 protein level has also been previously demonstrated in some lysosomal storage diseases in which the autophagic pathway is disturbed by mutations in lysosomal enzymes such as Niemann-Pick type C disease patients' fibroblasts (Pugach et al., 2018), Pompe disease patients' fibroblasts (Meikle et al., 1999), Cystinosis mouse model (Ctsn-/-) fibroblast cells and tissue samples (Napolitano et al., 2015). The elevated level of LAMP1 we demonstrated in this study may present the impaired autophagy-lysosomal system in the deficiency of catalytic

activity of lysosomal Cathepsin A. Determining whether the increased LAMP1 protein expression in CathA^{S190A} neuroglia and fibroblast cells indicates an increase in the number of lysosomes or is due to the higher number of LAMP1 presence in enlarged lysosomal membranes is difficult to explain with our results, so further investigations are needed to clearly explain the increased protein level of LAMP1 resulting from the catalytically deficient lysosomal Cathepsin A. In CathA^{S190A} neuroglia cells, compared to non-treated (None) condition, autophagy-inducing Starvation and Rapamycin+Starvation conditions have effectively reduced the elevated level of LAMP1 protein (Figure 3.6.A and C). On the other hand, all of the autophagy-inducing treatment conditions resulted in decreasing in the LAMP1 protein level in CathA^{S190A} fibroblast cells compared to the non-treated (None) condition (Figure 3.8.A and C). In conclusion, Starvation and Rapamycin+Starvation treatment conditions seem appropriate to significantly reduce the increased LAMP1 protein level in CathA^{S190A} neuroglia and fibroblast cells, as well as the degradation of accumulated LC3 and p62 proteins.

CHAPTER 5

CONCLUSION

In this study, I investigated whether the role of the catalytic activity of lysosomal Cathepsin A enzyme in the regulation of autophagic flux in neuroglia and fibroblast cells established from $CathA^{S190A}$ mouse which is a catalytically inactive Cathepsin A mouse model.

RT-PCR analyzes I performed in $CathA^{S190A}$ neuroglia and fibroblast cells with their $CathA^{+/+}$ counterparts for the autophagy marker genes which were Beclin-1, ATG9, ATG7, p62 and LAMP2, have demonstrated that deficiency of catalytic activity of lysosomal Cathepsin A enzyme leads to alterations in the expression profiles of autophagy marker genes. Additionally, these alterations in expression level were seen with $CathA^{S190A}$ neuroglia and $CathA^{S190A}$ cells showing different patterns compared to $CathA^{+/+}$ cells. In more detailed perspective, the expression levels of autophagy marker genes in both $CathA^{S190A}$ neuroglia and $CathA^{S190A}$ fibroblast cells were almost the same, whereas the basal expression levels of these genes in $CathA^{+/+}$ cells were very different and so, resulted in alterations with different patterns for these genes in the two different cell lines.

Western Blot and Immunocytochemistry analyses I performed have demonstrated that LC3, p62, and LAMP1 proteins accumulated significantly in neuroglia and fibroblast cells in the deficiency of catalytic activity of the lysosomal Cathepsin A enzyme. As mentioned above (Settembre et al., 2008; Fukuda et al., 2006), the secondary accumulation of these autophagic proteins is considered an indicator of impaired autophagic flux. In conclusion, we think that the catalytic activity of the lysosomal Cathepsin A enzyme plays a role in the proper completion of the autophagic flux in the cell. The impaired autophagic flux caused by the deficiency of the catalytic activity of the lysosomal Cathepsin A enzyme may be due to the inability to degrade the short bioactive peptides, which are known to be the substrate of the lysosomal Cathepsin A enzyme and accumulated in different tissues of $CathA^{S190A}$ mice, by autophagy at the cellular level.
We used Rapamycin, a chemical agent, starvation, which is a type of cellular stress, and a combination of these two conditions to restore the autophagic flux, which we showed

to be impaired at the cellular level in the deficiency of catalytic activity of lysosomal Cathepsin A enzyme. As a result of the analyzes we performed at the level of gene and protein expression, we decided that all the treatment conditions which were Rapamycin, Starvation, and Rapamycin+Starvation may effective in the clearance of the accumulated LC3, p62, and Lamp1 proteins in catalytically inactive CathA^{S190A} neuroglia and fibroblast cells.

5.1. Future Directions

To better understand the role of the catalytic activity of the lysosomal Cathepsin A enzyme in the regulation of autophagy, more detailed analyzes can be performed on the lysosomes and their functionalities in CathA^{S190A} neuroglia and fibroblast cells. It should be clarified that impaired autophagic machinery and incompleteness of autophagic flux in the deficiency of catalytic activity of lysosomal Cathepsin A enzyme is resulted from whether the inability of fusion of autophagosomes and lysosomes to form autophagolysosomes or inability to complete degradation of cellular autophagic cargoes and autophagic proteins in the autophagolysosomes.

The theory that the impaired autophagic flux caused by catalytically inactive Cathepsin A enzyme *in vitro* is due to this reason, should be strengthened by determining the protein levels of short bioactive peptides, which were previously shown to accumulate in different tissues of CathA^{S190A} mice. In addition, measuring the levels of these bioactive peptides under Starvation and Starvation+Rapamycin conditions, which have been shown to be effective in the repairing of impaired autophagic flux in CathA^{S190A} neuroglia and fibroblast cells, will also be important for a better understanding of short bioactive peptides' biology under autophagy-inducing conditions. In addition to this *in vitro* study, it may be required that analyze the autophagic flux *in vivo* in different age groups, especially in 5 different tissues of the CathA^{S190A} mice, which were previously shown to accumulate short bioactive peptides.

As a last, the basal level of chaperone-mediated autophagy in CathA^{S190A} neuroglia and fibroblast cells and in different tissues of the CathA^{S190A} mouse can also be analyzed because the role of Cathepsin A enzyme in chaperone-mediated autophagy was previously reported. Additionally, the levels of chaperone-mediated autophagy and macroautophagy in CathA^{S190A} neuroglia and fibroblast cells and in different tissues of

the CathA^{S190A} mouse may be analyzed comparatively to demonstrate whether there is any relation between 2 different types of autophagy such as compensatory or competitor relation.

REFERENCES

Annunziata I, d'Azzo A. Galactosialidosis: historic aspects and overview of investigated and emerging treatment options. *Expert Opin Orphan Drugs*. 2017;5(2):131-141.

Aschner M, Allen JW, Kimelberg HK, LoPachin RM, Streit WJ. Glial cells in neurotoxicity development. *Annu Rev Pharmacol Toxicol*. 1999;39:151-73

Birgisdottir ÅB, Johansen T. Autophagy and endocytosis - interconnections and interdependencies. *J Cell Sci.* 2020 May 22;133(10):jcs228114.

Bitto A, Lerner CA, Nacarelli T, Crowe E, Torres C, Sell C. P62/SQSTM1 at the interface of aging, autophagy, and disease. *Age (Dordr).* 2014 Jun;36(3):9626.

Bjørkøy G, Lamark T, Johansen T. p62/SQSTM1: a missing link between protein aggregates and the autophagy machinery. *Autophagy*. 2006 Apr-Jun;2(2):138-9.

Bonten EJ, Annunziata I, d'Azzo A. Lysosomal multienzyme complex: pros and cons of working together. *Cell Mol Life Sci*. 2014 Jun;71(11):2017-32.

Braulke T, Bonifacino JS. Sorting of lysosomal proteins. *Biochim Biophys Acta*. 2009 Apr;1793(4):605-14.

Breton C, Zingg HH. Expression and region-specific regulation of the oxytocin receptor gene in rat brain. *Endocrinology*. 1997 May;138(5):1857-62.

Brix, K. (2005). Lysosomal Proteases. In: Lysosomes. *Medical Intelligence Unit. Springer*, Boston, MA.

Calhan OY, Seyrantepe V. Mice with Catalytically Inactive Cathepsin A Display Neurobehavioral Alterations. *Behav Neurol*. 2017;2017:4261873.

Chévrier M, Brakch N, Céline L, Genty D, Ramdani Y, Moll S, Djavaheri-Mergny M, Brasse-Lagnel C, Annie Laquerrière AL, Barbey F, Bekri S. Autophagosome maturation is impaired in Fabry disease. *Autophagy*. 2010 Jul;6(5):589-99.

Cuervo AM, Mann L, Bonten EJ, d'Azzo A, Dice JF. Cathepsin A regulates chaperone-mediated autophagy through cleavage of the lysosomal receptor. *EMBO J*. 2003 Jan 2;22(1):47-59.

D'Azzo A, Hoogeveen A, Reuser AJ, Robinson D, Galjaard H. Molecular defect in combined beta-galactosidase and neuraminidase deficiency in man. *Proc Natl Acad Sci U S A*. 1982 Aug;79(15):4535-9.

Davenport AP, Hyndman KA, Dhaun N, Southan C, Kohan DE, Pollock JS, Pollock DM, Webb DJ, Maguire JJ. Endothelin. *Pharmacol Rev.* 2016 Apr;68(2):357-418.

Del Grosso A, Angella L, Tonazzini I, Moscardini A, Giordano N, Caleo M, Rocchiccioli S, Cecchini M. Dysregulated autophagy as a new aspect of the molecular pathogenesis of Krabbe disease. *Neurobiol Dis.* 2019 Sep;129:195-207.

Dennemärker J, Lohmüller T, Müller S, Aguilar SV, Tobin DJ, Peters C, Reinheckel T. Impaired turnover of autophagolysosomes in cathepsin L deficiency. *Biol Chem*. 2010 Aug;391(8):913-22.

Duve, C. de, B.C. Pressman, R. Gianetto, R. Wattiaux and F. Appelmans: Tissue Fractionation Studies. 6. Intracellular distribution patterns of enzymes in rat liver tissue. *Biochem. J*. 60, 604–617 (1955).

Duve, C. de: Lysosomes, a new group of cytoplasmic particles. In: Subcellular Particles (T. Hayashi, ed.), pp. 128–159. *New York: Ronald Press* 1959.

Eskelinen EL. Roles of LAMP-1 and LAMP-2 in lysosome biogenesis and autophagy. *Mol Aspects Med*. 2006 Oct-Dec;27(5-6):495-502.

Feng Y, He D, Yao Z, Klionsky DJ. The machinery of macroautophagy. *Cell Res*. 2014 Jan;24(1):24-41.

Fukuda T, Ewan L, Bauer M, Mattaliano RJ, Zaal K, Ralston E, Plotz PH, Raben N. Dysfunction of endocytic and autophagic pathways in a lysosomal storage disease. *Ann Neurol*. 2006 Apr;59(4):700-8.

Gorelik A, Illes K, Hasan SMN, Nagar B, Mazhab-Jafari MT. Structure of the murine lysosomal multienzyme complex core. *Sci Adv*. 2021 May 12;7(20):eabf4155.

Gump JM, Thorburn A. Autophagy and apoptosis: what is the connection? *Trends Cell Biol.* 2011 Jul;21(7):387-92.

Guo D, Zhang L, Wang X, Zheng J, Lin S. Establishment methods and research progress of livestock and poultry immortalized cell lines: A review. *Front Vet Sci*. 2022 Sep 2;9:956357.

He C, Klionsky DJ. Regulation mechanisms and signaling pathways of autophagy. *Annu Rev Genet*. 2009;43:67-93.

Hiraiwa M. Cathepsin A/protective protein: an unusual lysosomal multifunctional protein. *Cell Mol Life Sci*. 1999 Dec;56(11-12):894-907.

Ichimiya T, Yamakawa T, Hirano T, Yokoyama Y, Hayashi Y, Hirayama D, Wagatsuma K, Itoi T, Nakase H. Autophagy and Autophagy-Related Diseases: *A Review. Int J Mol Sci*. 2020 Nov 26;21(23):8974.

Ichimura Y, Komatsu M. Selective degradation of p62 by autophagy. *Semin Immunopathol*. 2010 Dec;32(4):431-6.

Itoh K, Oyanagi K, Takahashi H, Sato T, Hashizume Y, Shimmoto M, Sakuraba H. Endothelin-1 in the brain of patients with galactosialidosis: its abnormal increase and distribution pattern. *Ann Neurol.* 2000 Jan;47(1):122-6.

Jackman HL, Tan FL, Tamei H, Beurling-Harbury C, Li XY, Skidgel RA, Erdös EG. A peptidase in human platelets that deamidates tachykinins. Probable identity with the lysosomal "protective protein". *J Biol Chem*. 1990 Jul 5;265(19):11265-72.

Jackman HL, Morris PW, Deddish PA, Skidgel RA, Erdös EG. Inactivation of endothelin I by deamidase (lysosomal protective protein). *J Biol Chem*. 1992 Feb 15;267(5):2872-5.

Jennings JJ Jr, Zhu JH, Rbaibi Y, Luo X, Chu CT, Kiselyov K. Mitochondrial aberrations in mucolipidosis Type IV. *J Biol Chem*. 2006 Dec 22;281(51):39041-50.

King JS. Autophagy across the eukaryotes: is S. cerevisiae the odd one out? *Autophagy*. 2012 Jul 1;8(7):1159-62.

Laplante M, Sabatini DM. Regulation of mTORC1 and its impact on gene expression at a glance. *J Cell Sci*. 2013 Apr 15;126(Pt 8):1713-9.

Lee WS, Yoo WH, Chae HJ. ER Stress and Autophagy. *Curr Mol Med*. 2015;15(8):735-45.

Liao G, Yao Y, Liu J, Yu Z, Cheung S, Xie A, Liang X, Bi X. Cholesterol accumulation is associated with lysosomal dysfunction and autophagic stress in Npc1 -/- mouse brain. *Am J Pathol*. 2007 Sep;171(3):962-75.

Lieberman AP, Puertollano R, Raben N, Slaugenhaupt S, Walkley SU, Ballabio A. Autophagy in lysosomal storage disorders. *Autophagy*. 2012 May 1;8(5):719-30.

López-Otín C, Bond JS. Proteases: multifunctional enzymes in life and disease. *J Biol Chem*. 2008 Nov 7;283(45):30433-7.

Mari M, Tooze SA, Reggiori F. The puzzling origin of the autophagosomal membrane. F1000 *Biol Rep*. 2011;3:25

.

Meikle PJ, Yan M, Ravenscroft EM, Isaac EL, Hopwood JJ, Brooks DA. Altered trafficking and turnover of LAMP-1 in Pompe disease-affected cells. *Mol Genet Metab*. 1999 Mar;66(3):179-88.

Min Y, Xu W, Liu D, Shen H, Xu Y, Zhang S, Zhang L, Wang H. Earle's balanced salts solution and rapamycin differentially regulate the Bacillus Calmette-Guerin-induced maturation of human dendritic cells. *Acta Biochim Biophys Sin (Shanghai)*. 2013 Mar;45(3):162-9.

Mizushima N, Ohsumi Y, Yoshimori T. Autophagosome formation in mammalian cells. *Cell Struct Funct*. 2002 Dec;27(6):421-9.

Mizushima N, Yoshimori T, Levine B. Methods in mammalian autophagy research. *Cell*. 2010 Feb 5;140(3):313-26.

Mizushima N, Yoshimori T, Ohsumi Y. The role of Atg proteins in autophagosome formation. *Annu Rev Cell Dev Biol*. 2011;27:107-32.

Müller S, Dennemärker J, Reinheckel T. Specific functions of lysosomal proteases in endocytic and autophagic pathways. *Biochim Biophys Acta*. 2012 Jan;1824(1):34-43.

Myerowitz R, Puertollano R, Raben N. Impaired autophagy: The collateral damage of lysosomal storage disorders. *EBioMedicine*. 2021 Jan;63:103166.

Nascimbeni AC, Fanin M, Masiero E, Angelini C, Sandri M. The role of autophagy in the pathogenesis of glycogen storage disease type II (GSDII). *Cell Death Differ*. 2012 Oct;19(10):1698-708.

Napolitano G, Johnson JL, He J, Rocca CJ, Monfregola J, Pestonjamasp K, Cherqui S, Catz SD. Impairment of chaperone-mediated autophagy leads to selective lysosomal degradation defects in the lysosomal storage disease cystinosis. *EMBO Mol Med*. 2015 Feb;7(2):158-74.

Orsi A, Polson HE, Tooze SA. Membrane trafficking events that partake in autophagy. *Curr Opin Cell Biol*. 2010 Apr;22(2):150-6.

Pan X, Grigoryeva L, Seyrantepe V, Peng J, Kollmann K, Tremblay J, Lavoie JL, Hinek A, Lübke T, Pshezhetsky AV. Serine carboxypeptidase SCPEP1 and Cathepsin A play complementary roles in regulation of vasoconstriction via inactivation of endothelin-1. *PLoS Genet*. 2014 Feb 27;10(2):e1004146.

Parzych KR, Klionsky DJ. An overview of autophagy: morphology, mechanism, and regulation. *Antioxid Redox Signal.* 2014 Jan 20;20(3):460-73.

Platt, F.M., d'Azzo, A., Davidson, B.L. et al. Lysosomal storage diseases. *Nat Rev Dis Primers* 4, 27 (2018).

Pugach EK, Feltes M, Kaufman RJ, Ory DS, Bang AG. High-content screen for modifiers of Niemann-Pick type C disease in patient cells. *Hum Mol Genet*. 2018 Jun 15;27(12):2101-2112.

Pugsley HR. Assessing Autophagic Flux by Measuring LC3, p62, and LAMP1 Co-localization Using Multispectral Imaging Flow Cytometry. *J Vis Exp*. 2017 Jul 21;(125):55637.

Rokicki, J., Kaufmann, T., de Lange, AM.G. et al. Oxytocin receptor expression patterns in the human brain across development. *Neuropsychopharmacol*. 47, 1550–1560 (2022).

Runwal G, Stamatakou E, Siddiqi FH, Puri C, Zhu Y, Rubinsztein DC. LC3-positive structures are prominent in autophagy-deficient cells. *Sci Rep*. 2019 Jul 12;9(1):10147.

Russell RC, Tian Y, Yuan H, Park HW, Chang YY, Kim J, Kim H, Neufeld TP, Dillin A, Guan KL. ULK1 induces autophagy by phosphorylating Beclin-1 and activating VPS34 lipid kinase. *Nat Cell Biol*. 2013 Jul;15(7):741-50.

Sarkar, S., Ravikumar, B., Floto, R. et al. Rapamycin and mTOR-independent autophagy inducers ameliorate toxicity of polyglutamine-expanded huntingtin and related proteinopathies. *Cell Death Differ* 16, 46–56 (2009)

Sarkar S, Carroll B, Buganim Y, Maetzel D, Ng AH, Cassady JP, Cohen MA, Chakraborty S, Wang H, Spooner E, Ploegh H, Gsponer J, Korolchuk VI, Jaenisch R. Impaired autophagy in the lipid-storage disorder Niemann-Pick type C1 disease. *Cell Rep*. 2013 Dec 12;5(5):1302-15.

Sawa-Makarska J, Baumann V, Coudevylle N, von Bülow S, Nogellova V, Abert C, Schuschnig M, Graef M, Hummer G, Martens S. Reconstitution of autophagosome nucleation defines Atg9 vesicles as seeds for membrane formation. *Science*. 2020 Sep 4;369(6508):eaaz7714.

Sengul T, Can M, Ateş N, Seyrantepe V. Autophagic flux is impaired in the brain tissue of Tay-Sachs disease mouse model. *PLoS One*. 2023 Mar 16;18(3):e0280650.

Settembre C, Fraldi A, Rubinsztein DC, Ballabio A. Lysosomal storage diseases as disorders of autophagy. *Autophagy*. 2008 Jan;4(1):113-4.

Seyrantepe V, Hinek A, Peng J, Fedjaev M, Ernest S, Kadota Y, Canuel M, Itoh K, Morales CR, Lavoie J, Tremblay J, Pshezhetsky AV. Enzymatic activity of lysosomal carboxypeptidase (cathepsin) A is required for proper elastic fiber formation and inactivation of endothelin-1. *Circulation*. 2008 Apr 15;117(15):1973-81.

Seyrantepe V, Demir SA, Timur ZK, Von Gerichten J, Marsching C, Erdemli E, Oztas E, Takahashi K, Yamaguchi K, Ates N, Dönmez Demir B, Dalkara T, Erich K, Hopf C, Sandhoff R, Miyagi T. Murine Sialidase Neu3 facilitates GM2 degradation

and bypass in mouse model of Tay-Sachs disease. *Exp Neurol*. 2018 Jan;299(Pt A):26-41.

Sun Y, Grabowski GA. Impaired autophagosomes and lysosomes in neuronopathic Gaucher disease. *Autophagy*. 2010 Jul;6(5):648-9.

Tanaka Y, Guhde G, Suter A, Eskelinen EL, Hartmann D, Lüllmann-Rauch R, Janssen PM, Blanz J, von Figura K, Saftig P. Accumulation of autophagic vacuoles and cardiomyopathy in LAMP-2-deficient mice. *Nature*. 2000 Aug 24;406(6798):902-6.

Tanida I, Ueno T, Kominami E. LC3 conjugation system in mammalian autophagy. *Int J Biochem Cell Biol*. 2004 Dec;36(12):2503-18.

Timur ZK, Akyildiz Demir S, Seyrantepe V. Lysosomal Cathepsin A Plays a Significant Role in the Processing of Endogenous Bioactive Peptides. *Front Mol Biosci*. 2016 Oct 25;3:68.

Vergarajauregui S, Connelly PS, Daniels MP, Puertollano R. Autophagic dysfunction in mucolipidosis type IV patients. *Hum Mol Genet.* 2008 Sep 1;17(17):2723-37.

Yadati T, Houben T, Bitorina A, Shiri-Sverdlov R. The Ins and Outs of Cathepsins: Physiological Function and Role in Disease Management. *Cells*. 2020 Jul 13;9(7):1679.

Yang Z, Klionsky DJ. Eaten alive: a history of macroautophagy. *Nat Cell Biol*. 2010 Sep;12(9):814-22.

Yang M, Liu J, Shao J, Qin Y, Ji Q, Zhang X, Du J. Cathepsin S-mediated autophagic flux in tumor-associated macrophages accelerate tumor development by promoting M2 polarization. *Mol Cancer*. 2014 Mar 2;13:43.

Yim WW, Mizushima N. Lysosome biology in autophagy. *Cell Discov*. 2020 Feb 11;6:6.

Yoshii SR, Mizushima N. Monitoring and Measuring Autophagy. *Int J Mol Sci*. 2017 Aug 28;18(9):1865.

Yu L, Chen Y, Tooze SA. Autophagy pathway: Cellular and molecular mechanisms. *Autophagy*. 2018;14(2):207-215.